Received: 4 April 2024 | Accepted: 27 August 2024

DOI: 10.1111/1462-2920.16698

BRIEF REPORT

ENVIRONMENTAL MICROBIOLOGY

Specialization of *Alcanivorax* species in colonizing diverse plastics

Valérie Mattelin[1] | **Astrid Rombouts**[1] | **Josefien Van Landuyt**[1] | **Alberto Scoma**[2] | **Nico Boon**[1,3]

[1]CMET, Universiteit Gent, Ghent, Belgium

[2]EMS Laboratory, Section of Biological and Chemical Engineering (BCE), Department of Engineering, Aarhus University, Aarhus, Denmark

[3]Centre for Advanced Process Technology for Urban Resource Recovery (CAPTURE), Ghent, Belgium

Correspondence
Nico Boon, Ghent University, Faculty of Bioscience Engineering, Centre for Microbial Ecology and Technology (CMET), Coupure Links 653, B-9000 Gent, Belgium.
Email: nico.boon@ugent.be

Funding information
Bijzonder Onderzoeksfonds UGent, Grant/Award Number: BOF.BAS.2022.0014.01; Agentschap Innoveren en Ondernemen, Grant/Award Number: HBC.2019.2622; Fonds Wetenschappelijk Onderzoek, Grant/Award Numbers: 1288224N, 1S24323N

Abstract

Recently, there has been increased attention to hydrocarbonoclastic bacteria in the plastisphere. One particular genus, *Alcanivorax*, is reported in the biodegradation of several polymers in the literature. In this study, we further explored the role of *Alcanivorax* in the early colonization of poly(3-hydroxybutyrate-co-3-hydroxyhexanoate) (PHBH), nylon 6/69, and a novel plastic B4PF01. Starting from enrichments of a one-year experiment with a maximum relative abundance of 58.8% of *Alcanivorax*, two parallel experiments were set up. One experiment followed growth and activity during the first 21 days of plastic incubations, and the other followed the same parameters on the different material fractions of the plastics, such as leachables and pure polymer. For all plastic types, the highest microbial growth was associated with the total plastics compared to the other material fractions. A relative abundance of 62.7% of *Alcanivorax* in the nylon 6/69-enriched community was observed. This, combined with data on activity, suggests that nylon 6/69 is potentially degraded by this genus. Two isolates were obtained, closely related to *A. borkumensis* SK2 and *Alcanivorax* sp. DG881. The activity and growth of the isolates as axenic cultures resemble their abundance in the community. In conclusion, this study contributes to the knowledge of the role of *Alcanivorax* in plastic-enriched communities.

INTRODUCTION

Marine plastic pollution is a worldwide problem, affecting organisms living in aqueous environments as well as (indirectly) terrestrial life. As their presence implies interactions between microorganisms and polymer surfaces, much research is devoted to plastic colonization and biodegradation by microorganisms. It is well-reported that microorganisms in aqueous environments form biofilms on a variety of solid surfaces, including plastics. In the case of plastic, this is referred to as plastisphere (Bryant et al., 2016; De Tender et al., 2015; De Tender et al., 2017; Dussud et al., 2018; Jacquin et al., 2019; Kirstein et al., 2019; Schlundt et al., 2020; Zettler et al., 2013). While it is clear that microorganisms attached to particulate organic matter degrade these organic compounds (Datta et al., 2016; Ebrahimi et al., 2019), the exact role of microorganisms attached to plastics is not yet elucidated or has even been considered negligible (Oberbeckmann & Labrenz, 2020). They can be present in the plastisphere for (1) attached lifestyle on a (hydrophobic) physical growth support, (2) chemoattraction towards leached dissolved organic matter (including hydrocarbons), (3) utilization of absorbed organic matter adsorbed on the surface, (4) metabolic incentives as cheater species or (5) active plastic-degradation function (Bos et al., 2023; Delacuvellerie

Valérie Mattelin and Astrid Rombouts contributed equally to this study.

et al., 2022). Their presence could cover multiple incentives and vary over time as the formation of plastisphere on plastic surfaces occurs in different phases and microbial successions have been observed (Bos et al., 2023; Dussud, Hudec, et al., 2018; Schefer et al., 2023; Wallbank et al., 2022). However, detailed research on the early stages of microbial colonization on plastics and the growth dynamics is still missing (Sun et al., 2023).

Hydrocarbonoclastic bacteria are often reported in plastic biodegradation studies (Wright, Langille, & Walker, 2021). Plastics can leach additives or readily available monomers and oligomers, that can act as an energy source and as a chemoattractant for some microorganisms. When these leachables are short alkanes, there will likely be a selective advantage for hydrocarbonoclastic bacteria and as such, the marine microbial community will restructure (Dey et al., 2022; Focardi et al., 2022; Romera-Castillo et al., 2018). However, due to the often lipophilic character of some of the leached compounds, they can also inhibit microbial activity (Costa et al., 2023; Focardi et al., 2022). Furthermore, it has been suggested that this effect is only present at earlier stages during microbial colonization (Erni-Cassola et al., 2020; Wright, Langille, & Walker, 2021).

It has been reported that obligate hydrocarbonoclastic bacteria (OHCB) possess a less restricted metabolic versatility than only hydrocarbon compounds (Radwan et al., 2019; Yakimov et al., 2022). *Alcanivorax*, as well as other OHCBs such as *Oleispira* and *Cycloclasticus* spp., have numerous enzymes that are reported to be active on different types of polyesters and encode other enzymes that potentially can be active on aliphatic polyesters (Roager & Sonnenschein, 2019; Yakimov et al., 2022). More specifically, an *Alcanivorax* isolate from the North Atlantic Ocean was capable of degrading polyhydroxybutyrate (PHB) by PHB depolymerase (PhaZ) (Cao et al., 2022), and also PHAs in general (Zhang et al., 2024). A different species from this genus, *Alcanivorax borkumensis*, has been suggested as the primary plastic degrader for low-density polyethylene (LDPE) in a microbial community, utilizing both the leachables and the polymer (Delacuvellerie et al., 2019; Zadjelovic et al., 2022). However, the recurring presence of *Alcanivorax* and other hydrocarbonoclastic bacteria on different types of plastic indicates that the full metabolic versatility has not yet been explored.

Driven by the observation of high relative abundances of *Alcanivorax* in our enrichments on different types of plastic (and in controls without plastic) and its reported active role in the biodegradation of several other polymers, more effort was put into elucidating its role in the early colonization of plastics. Additionally, a distinction was made between the different carbon fractions that are present in plastic, namely, leachables and pure polymer, to discover the utilization of all fractions as carbon sources.

In short, this research investigates to what extent the high abundance of the genus *Alcanivorax* correlates with early colonization (21 days) of different plastic types in both axenic cultures (isolated from the enriched communities) and as members of an enriched community (schematic representation is given in Figure 1). Three types of plastic and associated plastic-enriched communities were used, namely, (1) B4PF01, a novel plastic, (2) nylon 6/69, considered a non-biodegradable plastic (Tokiwa et al., 2009) and (3) Poly(3-hydroxybutyrate-co-3-hydroxyhexanoate) (PHBH), a biodegradable plastic (*KANEKA Biodegradable Polymer Green Planet*™ | KANEKA, n.d.). Next to growth, four complementary methods were used for analysing the community composition characteristics, (1) BONCAT, indicating the proportion of the microbial community that is actively synthesizing proteins, (2) FISH, indicating the *Alcanivorax* population with high ribosomal content, (3) BONCAT-FACS (fluorescent activated cell sorting) combined with 16S rRNA gene amplicon sequencing of the protein synthesizing population and (4) 16S rRNA gene amplicon sequencing of the total community. In addition to the total plastics, a biodegradation experiment, analysing dissolved organic carbon (DOC) concentration, was set up in which it was investigated whether the colonization and biodegradation capability of the enriched microbiome differs when exposed to leachables versus the pure polymer, and what role *Alcanivorax* plays in utilizing the different carbon sources. Leachables are defined as the residual monomeric and oligomeric compounds as the plastics in this study do not contain additives, the pure polymer is material without leachable compounds in the matrix, and total plastics are the original material, containing leachable and pure polymer. Last, the two newly isolated *Alcanivorax* strains from the enriched communities were compared to each other and the original enriched community in terms of growth rates and metabolic activity. Additionally, it was verified whether the isolated *Alcanivorax* strains were conclusively linked to the original plastisphere, as confirmed by placing their 16S rRNA gene amplicon sequences and the 16S rRNA gene amplicon sequencing data of the original enrichments in a phylogenetic tree.

EXPERIMENTAL PROCEDURES

Media preparation and plastic supply

The media used in the setup were mineral salts medium without carbon, adapted from Stanier et al. (1966), by elimination of all carbon, ONR7a and marine broth (MB 2216, Difco). For the mineral salts medium,

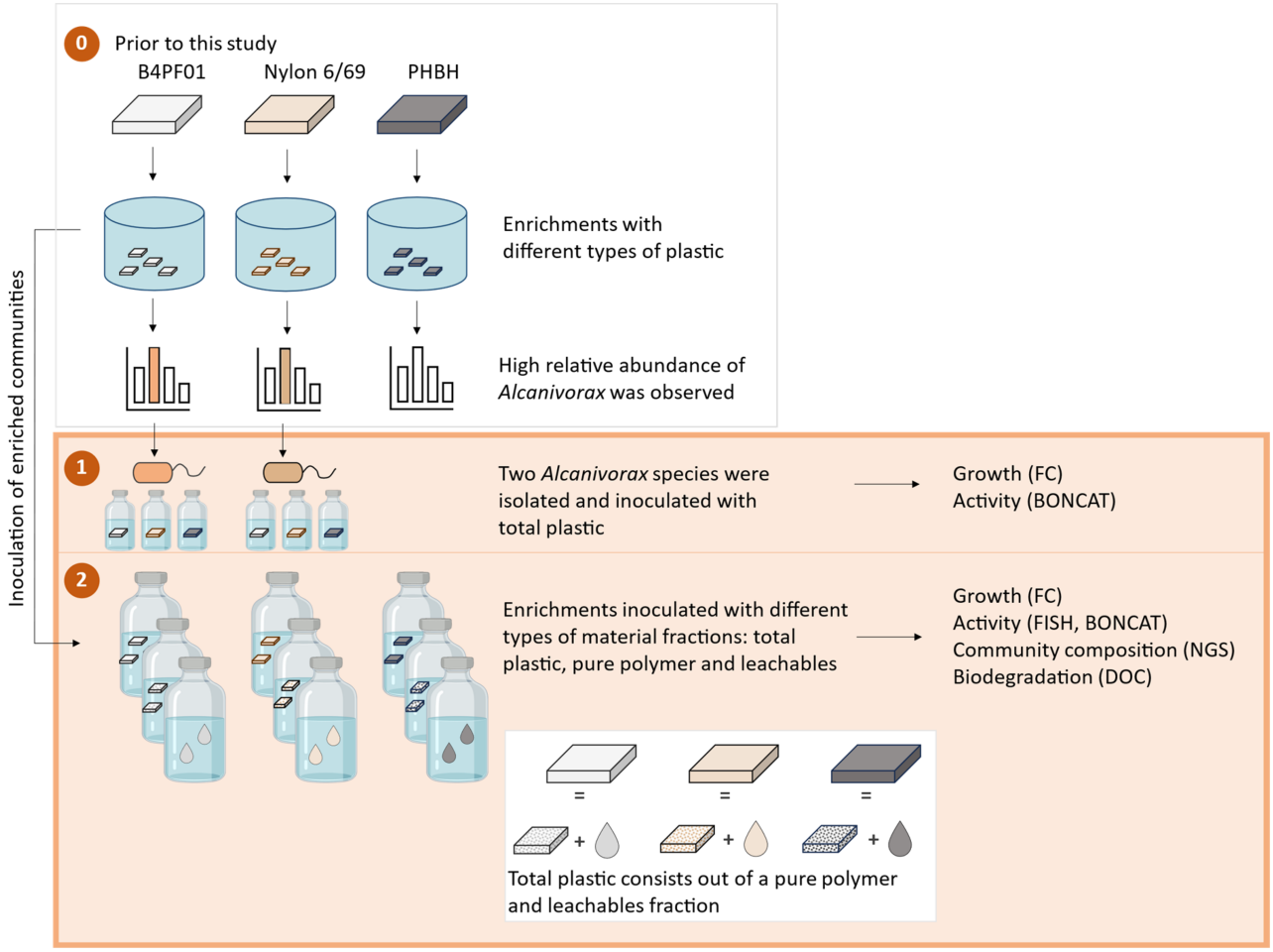

FIGURE 1 Experimental plan of this research. (A) Prior to this research, enrichment experiments were conducted with different types of plastics. By 16S rRNA gene amplicon sequencing, the high relative abundance of the genus *Alcanivorax* was remarked. (B) The enriched *Alcanivorax* species were isolated from the different enrichments and their growth and activity on total plastics was investigated. (C) The enriched communities were inoculated with total plastics, pure polymer or leachables material fractions. Growth, activity and community composition were investigated for the plastic-enriched microbial communities and the isolates on total plastics. Growth, activity and biodegradation by DOC were additionally investigated for the pure polymer and leachable fractions. FC, flow cytometry; FISH: fluorescent in situ hybridisation; BONCAT: biorthogonal non-canonical amino acid tagging; NGS: next-generation sequencing; DOC: dissolved organic carbon.

10 mL of a 1 M stock solution of Na_2HP0_4 and KH_2P0_4 was mixed with 3 mL of a 100 g/L stock solution of $(NH_4)_2S0_4$, 5 mL of a 19.7 g/L stock solution of $MgSO_4$, 5 mL of a 1.150 g/L stock solution $CaCl_2{\cdot}2H_2O$ and 5 mL of a trace elements solution (containing 0.640 g/L ETDA, 0.230 g/L $ZnSO_4{\cdot}7H_2O$, 0.550 g/L $FeSO_4{\cdot}7H_2O$, 0.340 g/L $MnSO_4{\cdot}H_2O$, 0.075 $CuSO_4{\cdot}5H_2O$ and 0.025 g/L $(NH_4)_6Mo_7O_{24}{\cdot}4H_2O$) and diluted in to a total volume of 1 L in 35 g/L artificial seawater (Instant Ocean®, Aquarium Systems, Mentor, OH, USA). ONR7a was prepared following the protocol from DSMZ (2007). The three different solutions were prepared and sterilized separately, and mixed afterwards. The pH of solution 1 was adjusted to 7.6 with NaOH. Solutions 1 and 2 were autoclaved, while solution 3 was sterilized by filtering (0.22 μm).

Model plastic types were chosen to represent three different categories: (A) novel plastic polymers (received from B4plastics), (B) non to hard-to-biodegrade plastic and (C) biodegradable plastic. The polymers used in this study are a polymer supplied by the company B4Plastics (Belgium) in category A, Polyamide 6/69 (PA 6/69, trivial name nylon 6/69) for category B and poly(3-hydroxybutyrate-co-3-hydroxyhexanoate) PHBH (Green Planet™ X331N, Kaneka biopolymers, USA) for category C. The chemical structure of the former polymer (referred to as B4PF01) is confidential. To increase biodegradability, it contains 0% ester bonds and 33% amide bonds.

Plastic enrichments

The enrichment procedure is described in Appendix A. Samples from these enrichments were taken as inoculum for the experiment described in this article.

Isolation campaign

Dilution to extinction was performed on the trickling filter enrichments with B4PF01, and flask enrichments with nylon 6/69 that showed a high relative abundance of *Alcanivorax* (Figure A1). After a total cell count of the communities stained with SG using Attune™ Nxt flow cytometer (Fisher Scientific™, Germany), the cells were diluted in series of 10-, 5- and 2-folds, up to 1 cell/mL. This was done in autoclaved glass test tubes filled with 4 mL ONR7a and 1% (vol/vol) C12. To define the uniformity of the cells, the samples were examined under the light microscope (Axioscope Zeiss, Germany). Once two dilution steps were performed in liquid media, the cells were also inoculated on solid plates of MB or ONR7a with 10 μL C16 on top. All dilution steps (four in liquid medium, four on solid ONR7a and six on solid MB) were performed in a sterile environment and all media were autoclaved or 0.22 μm filtered sterilized. In the case of liquid medium, a negative control was included in every dilution step to verify whether no contamination was induced. The incubation took place in the dark for 7 up to 10 days, at 20°C for both solid and liquid media and at 125 rpm for the liquids. The final classification of the pure cultures was performed with Sanger sequencing (full 16S, using universal bacterial primers 27F 5′ GAGTTTGATCMTGGCTCAG 3′ and 1492R 5′ GGYTACCTTGTTACGACTT 3′), after DNA extraction with phenol/chloroform or colony PCR.

Experimental setup

To obtain different fractions of the plastic, the plastic was incubated in an instant ocean® medium (salt mixture without phosphates and nitrates mimicking seawater) for 11 days at 20°C and 125 rpm. We assumed that the leaching reached a plateau after 11 days, as reported in other studies (Klaeger et al., 2019; Romera-Castillo et al., 2018). The polymer was separated from the building blocks by 0.22 μm filtration and subsequently rinsed 3× with instant ocean.

Flasks containing 20 mL mineral medium and 1 g/L of material fraction (i.e., total plastics, pure polymer or leachates)were inoculated with 10^5 cells/mL of the corresponding enrichment or isolate. Control flasks contained either only mineral medium, only the carbon fraction (abiotic control), or only microorganisms (control without carbon). The flasks were incubated at 20°C and 125 rpm. For each sampling time point, three replicates were prepared. Samples were vortexed for 30 s prior to sampling. Samples were taken on specific days, based on the acquired growth curves, and split in aliquots for fixation with 0.1% glutaraldehyde, fixation with 4% paraformaldehyde (PFA 4%) in ratio 1:3 sample:PFA, DNA extraction, dissolved organic carbon measurements if applicable and for bio-orthogonal non-canonical amino acid tagging (BONCAT) (Table 1). Control samples were taken less frequently as they represented undisturbed control conditions.

Microbial community analyses

Flow cytometry

Flow cytometry analysis of the glutaraldehyde fixed samples was performed by diluting the samples in 0.22 μm-filtered phosphate-buffered saline (PBS) buffer and staining with 1 vol% SYBR® Green I (SG, 100× concentrate in 0.22 μm-filtered DMSO, Invitrogen) for total cell analysis and staining with 1 vol% SYBR® Green I (SG, 100× concentrate in 0.22 μm-filtered DMSO, Invitrogen) mixed with 1 vol% propidium iodide (PI, 20 mM concentrate in 0.22 μm-filtered DMSO, Invitrogen) for intact/damaged cell analysis in three technical replicates.

Staining was performed with an incubation period of 20 min at 37°C in the dark. Samples were analysed immediately after incubation on an Attune™ Nxt flow cytometer (Fisher Scientific™, Germany) equipped with a blue (488 nm) and a red (637 nm) laser, with Attune focusing fluid (Fisher Scientific™, Germany) as sheath fluid. The instrument performance was verified daily using Attune performance tracking beads (Fisher Scientific™, Germany).

Bio-orthogonal non-canonical amino acid tagging (BONCAT)

Samples were incubated with 50 μM L-homopropargylglycine (HPG, 30 mM in Milli-Q™, 0.22 μm filter sterilized, Jena Bioscience) as amino acid analogue 3 h prior to sampling. Up to 200 μL of PFA fixed sample was vacuum filtered per well in a 96-well filter plate (MultiScreenHTS GV Filter Plate, 0.22 μm, opaque, non-sterile, Merck, Belgium), re-suspended in 200 μL 80% ethanol (0.22 μm filter sterilized) and incubated for 5 min at room temperature for dehydration. The ethanol was then removed through vacuum filtration. The same steps were repeated with 90% ethanol (0.22 μm filter sterilized). The cell pellets were re-suspended in 110.5 μL PBS, after which 6.25 μL 100 mM fresh aminoguanidine hydrochloride solution, 6.25 μL 100 mM fresh sodium ascorbate solution and 2.025 μL Click-it dye mix (Table 2) were added. This cell mixture was then incubated in a 96-well plate shaker (MB100-4A Thermo Shaker Allsheng, China) in the dark (25°C, 100 rpm) for 30 min. After incubation, all reagents were vacuum filtered and the cell pellet was washed three times with PBS (re-suspended in PBS, vacuum filtered; 3×). Depending on the cell concentration, the cell pellet

was diluted in up to 200 μL PBS. After this step, flow cytometric measurements were performed.

Bio-orthogonal non-canonical amino acid tagging (BONCAT)-sorting

The fixed sample was centrifuged for 5 min at maximal speed (20,238 rcf), after which the supernatant was removed. The cell pellet was re-suspended in 200 μL 80% ethanol and incubated for 3 min at room temperature for dehydration. The sample was centrifuged for 5 min at maximal speed and the supernatant was removed. The same steps were repeated with 90% ethanol, but in this case, 1 mL was added to the cell pellet. The cell pellet was re-suspended in 221 μL PBS, after which 12.5 μL 100 mM fresh aminoguanidine hydrochloride solution, 12.5 μL 100 mM fresh sodium ascorbate solution and 4.05 Click-it dye mix (Table 2) were added. This cell mixture was then incubated in a 96-well plate shaker (MB100-4A Thermo Shaker Allsheng, China) in the dark (25°C, 100 rpm) for 30 min up to 1.5 h. After incubation, the sample was centrifuged for 5 min at maximal speed and all supernatans were removed. The cell pellet was washed three times with PBS (re-suspended in PBS, centrifuged; removed supernatant; 3×). Depending on the cell concentration, the cell pellet was re-suspended in up to 200 μL of PBS. Counterstaining was performed with 1 vol% propidium iodide (PI, 20 mM concentrate in 0.22 μm-filtered DMSO, Invitrogen), 20 min in the dark. After this step, cell sorting was performed with a FACS Melody (BD, Erembodegem, Belgium) equipped with two lasers (488 nm blue and 562 nm yellow/green), with FACS Sheath (BD, Erembodegem, Belgium) as sheath fluid. The instrument performance was verified daily using CS&T RUO beads (BD, Erembodegem, Belgium).

Fluorescent in situ hybridization

Up to 200 μL of fixed sample was vacuum filtered, re-suspended in 100 μL 100% ethanol and incubated for 5 min at room temperature for dehydration. The ethanol was subsequently removed through vacuum filtration after which the cell pellet was air dried. 100 μL of hybridization buffer at 20% (vol/vol) formamide stringency (Table 3) was added onto the cell pellet together with 1 μL of the *Alcanivorax* probe (5′ CGA CGC GAC CTC ATC CAT CA 3′, Eurogentec, Belgium). Afterwards, the entire mixture was incubated in the hybridization oven at 46°C for 3 h. In the meantime, the washing buffer of the corresponding 20% formamide stringency (Table 3) was preheated to 48°C. After hybridization, the mixture was vacuum filtered and the cell pellet was re-suspended in 100 μL of the preheated washing buffer. This was incubated for 15 min at 48°C, followed by vacuum filtration. The cell pellet was re-suspended in up to 200 μL of PBS. Finally, flow cytometry was performed.

DNA extraction and Illumina sequencing

DNA extraction was performed with the DNeasy PowerSoil Pro Kit (Qiagen, Germany).

Successful DNA extraction was confirmed by PCR. The PCR product and the DNA extract were visualized on a 2% agarose gel. The genomic DNA of the enrichment samples was sent out to LGC Genomics GmbH (Berlin, Germany) for 16S rRNA gene V3–V4 hypervariable regions amplification by PCR using primers 341F (5′-CCT ACG GGN GGC WGC AG-3′) and 785Rmod (5′-GAC TAC HVG GGT ATC TAA KCC-3′) (Klindworth et al., 2013), for library preparation and sequencing on an Illumina Miseq platform with v3 chemistry.

Analytical techniques

Dissolved organic carbon

Samples for dissolved organic carbon were diluted in Milli-Q water (Merck, Belgium) and filtered over 0.22 μm in AOC-free vials, prepared according to Hammes and Egli (2005). Samples were analysed in a Sievers 900 Series Total Organic Carbon Analyser (GE Analytical instruments, PMT Benelux, Kampenhout, Belgium). The oxidizer flow rate was adjusted to the organic load of the sample. Samples were measured in four technical replicates.

Data analysis

Amplicon sequencing data

All data analysis was performed in R (version 4.0.3). The DADA2 R package was used to process the amplicon sequence data according to the pipeline tutorial (Callahan et al., 2016). In the first quality control step, the primer sequences were removed and reads were truncated at a quality score cut-off (truncQ = 2). Besides trimming, additional filtering was performed to eliminate reads containing any ambiguous base calls or reads with high expected errors (maxEE = 2.2). After dereplication, unique reads were further denoised using the Divisive Amplicon Denoising Algorithm (DADA) error estimation algorithm and the selfConsist sample inference algorithm (with the option pooling = TRUE). The obtained error rates were inspected and after approval, the denoised reads were merged. Finally, the ASV table obtained after chimaera removal was used

for taxonomy assignment using the Naive Bayesian Classifier and the DADA2 formatted Silva v138.1 (Quast et al., 2013).

Phylogenetic tree construction and evolutionary placement algorithm

To have a more in-depth characterization of the ASVs classified as *Alcanivorax* by Silva v138, the short reads were inserted into the best full-length reference tree using the RAxML evolutionary placement algorithm (EPA) (v 8.2.12) (Stamatakis, 2014) and the epa-ng algorithm (v0.2.1-beta) (Barbera et al., 2019), analogous to Mariën et al. (2022) and Prévoteau et al. (2021). The reference tree was built with the best hits of EZBioCloud (Yoon et al., 2017). A BLAST search of the ASVs, full 16S, with *Pseudomonas abietaniphila* as outgroup. The tree was visualized in iTOL (Letunic & Bork, 2019).

Statistical data analysis

Further data analysis was performed (R Core Team, 2020) using statistical packages. *Phyloseq* (v1.22.3) (McMurdie & Holmes, 2013) was used for amplicon sequencing data, *Phenoflow* (v1.1.2) (Props et al., 2016) for flow cytometry data, *growthcurver* (v 0.3.1) (Sprouffske & Wagner, 2016) for growth parameters and *vegan* (v2.5.6) (Dixon, 2003) for diversity analysis. The growth model used was the logistic equation, describing the population size $N(t)$ as a function of time by Equation (1), using the population size at the beginning ($N0$), the carrying capacity (K) and the growth rate (μ):

$$N(t) = \frac{K}{1 + \left(\frac{K - N0}{N0}\right) e^{-\mu t}}. \quad (1)$$

To assess significant changes due to the imposed environmental conditions, a *t*-test was used if assumptions were met and Wilcoxon rank sum tests were used when data was not normally distributed, using a cut-off of (adjusted) *p*-value >0.05.

RESULTS

Enriching for plastic-degrading microorganisms in the marine environment

Prior to this study, an enrichment experiment was set up to select for plastic-degrading microorganisms in the marine environment. Therefore, the indigenous microbiome of the North Sea (at the coast in Ostend, Belgium (51°10′31.1″ N; 3°14′00.6″ E)) was incubated with different types of plastics as the only carbon source in a batch flask experiment. After 1 year of flask enrichment, some of the mixed cultures (cultures grown on PHBH and B4PF01 plastics) were transferred to trickling filter bioreactor systems to promote biofilm growth for 5 months. The community composition was investigated in both types of enrichments (flasks and trickling filter). A remarkable dominance of the genus *Alcanivorax* was observed with 58.8% for B4PF01 trickling filter enrichments (Figure A1B) and 32.9% for nylon 6/69, flask enrichments (Figure A1A).

Microbial growth and activity on different types of plastic

To obtain insight into the growth of the total microbial communities on the three plastics (B4PF01, nylon 6/69 and PHBH), the enriched communities (trickling filter for B4PF01, flask for nylon 6/69 and PHBH) were re-inoculated in fresh medium at starting concentrations of 1×10^5 cells/mL and monitored using flow cytometry over an incubation period of 21 days. As carbon source, three material fractions of these three plastics were added, to investigate whether the enriched microbiome was able to use solely leached compounds, pure polymer or total plastics.

For the three plastics, growth is observed in all conditions, with the highest cell numbers for the total plastics fraction ($4.9 \times 10^6 \pm 2.3 \times 10^6$ cells/mL for B4PF01, $1.6 \times 10^7 \pm 5.9 \times 10^6$ cells/mL for nylon 6/69 and $3.0 \times 10^7 \pm 1.1 \times 10^7$ cells/mL for PHBH) (Figure 2). For all plastics, the mean cell concentration at 21 days is significantly higher for the total plastics fraction than the other conditions (Wilcoxon test, $p = 0.003$ and 0.002, for total plastics fraction of B4PF01 versus leachables and pure polymer fraction respectively, and $p < 0.001$ for total nylon 6/69 and PHBH versus corresponding leachables fraction, pure polymer fraction and no carbon), and higher, but not significantly higher, for B4PF01 versus no carbon control (Wilcoxon test, $p = 0.05$). Comparing the microbial growth on the three types of plastics, PHBH has the highest carrying capacity (i.e., the maximum microbial concentration that the medium including carbon source can carry and sustain), followed by nylon 6/69 and B4PF01, as determined by the four-parametric logistic growth model (Table 4). The cell concentrations on nylon 6/69 at Day 21 are higher for the control without a carbon source added (no carbon) compared to incubations with the leachable and the pure polymer fraction. Controls without microorganisms added confirmed no to low growth (Figure A2), except for nylon 6/69 pure polymer incubation (Figure 2).

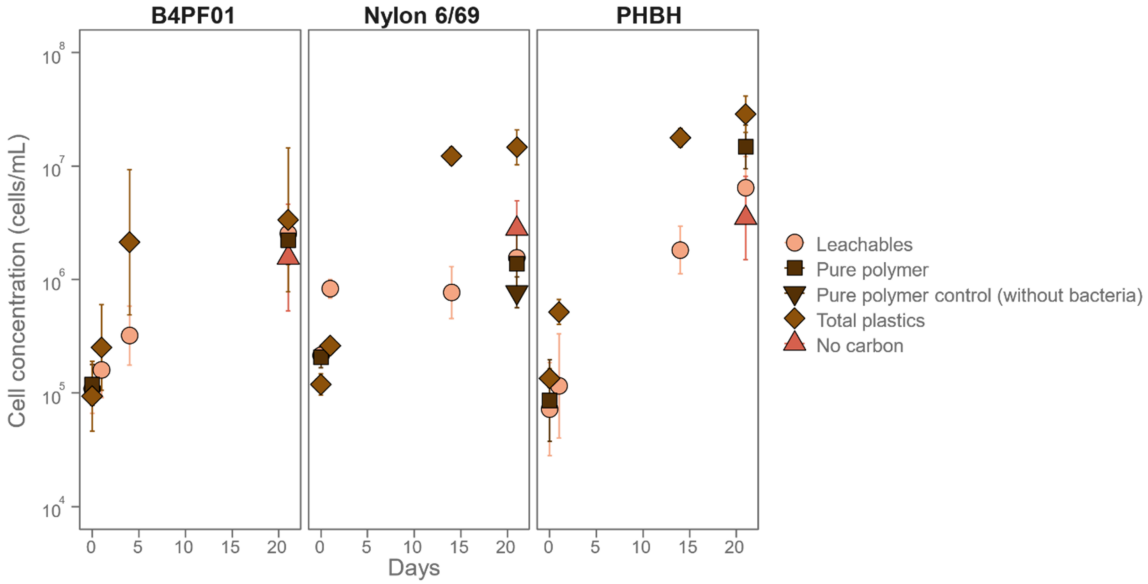

FIGURE 2 Cell growth of plastic-enriched communities on different types (B4PF01, nylon 6/69 and PHBH) and material fractions (leachables, pure polymer and total plastics (i.e., leachables + polymer)) of plastics during 21 days ($n = 3$, three technical replicates per biological triplicate as mean value, including standard deviation). 'Pure polymer control' indicates the incubation without microorganisms (only depicted for nylon 6/69, as concentration >10^5), and 'no carbon' indicates incubation of the microbial community without an added (plastic) carbon source. The gating strategy is shown in Figure A5.

TABLE 1 Maximum growth rate and carrying capacity of plastic communities on different types of plastics determined by the four-parametric logistic growth model.

	Growth rate (day^{-1})			Carrying capacity (cells/mL)		
	B4PF01	Nylon 6/69	PHBH	B4PF01	Nylon 6/69	PHBH
Total plastics	1.622	0.321	0.181	3.3×10^6	1.5×10^7	3.2×10^7
No carbon	0.301	0.601	0.505	2.5×10^6	3.0×10^6	4.0×10^6

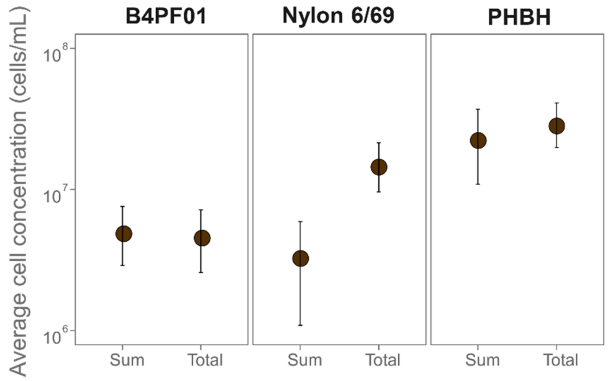

FIGURE 3 Cell concentrations at day 21 of fractions leachable and pure polymer summed and compared to the fraction of the total plastic ($n = 3$, standard deviation is shown).

When the cell concentrations obtained from the leachable and the pure polymer fractions are summed, they add up to the cell concentration in the total plastic fractions for B4PF01 and PHBH, but not for nylon 6/69 (Figure 3). This is confirmed statistically (Wilcoxon test, B4PF01: $p = 1$; nylon 6/69: $p < 0.001$; PHBH: $p = 0.1694$).

To investigate the substrate-dependency of the microbial communities further, the activity of the cells was analysed using bioorthogonal non-canonical amino acid tagging (BONCAT). The incorporation of amino acid analogues using BONCAT in combination with flow cytometry can distinguish the individual cells that actively synthesize proteins from the non-active ones.

The relative abundance of cells actively synthesizing proteins of the plastic communities peaks at 90.6% ± 3.1%, 90.8% ± 4.9% and 90.2% ± 6.1% for the total plastics fraction of respectively B4PF01, nylon 6/69 and PHBH after 4 days of growth (Figure 4). At Day 21, around 50% of the cells are still synthesizing proteins, for all material fractions and types of plastics, except for leachables (15.1% ± 8.6%) and pure polymer (18.4% ± 17.6%) of nylon 6/69.

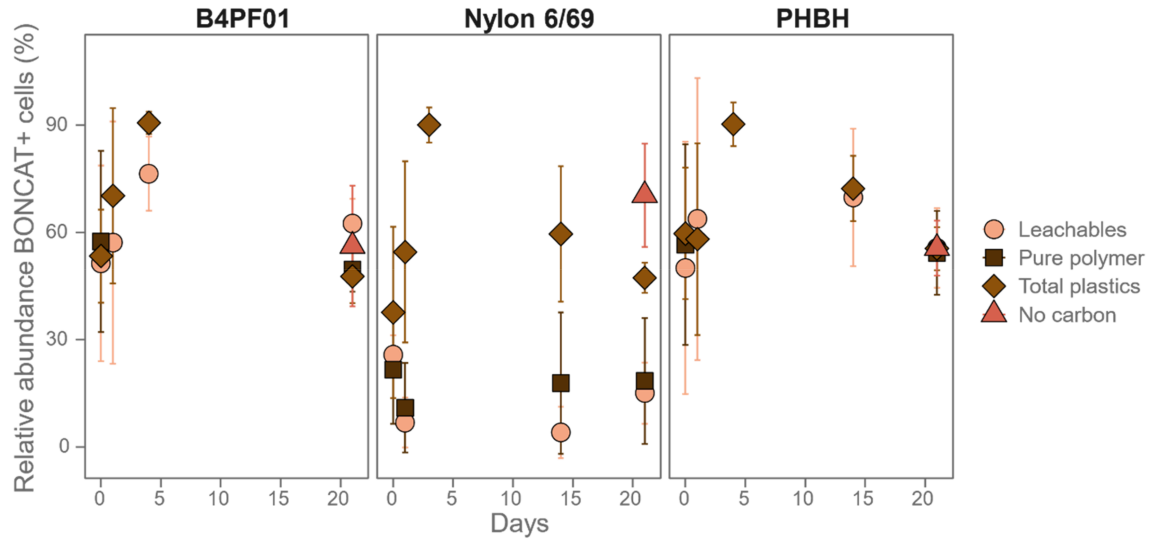

FIGURE 4 The average percentage of BONCAT+ cells within the community, indicating protein synthesis, on different types (B4PF01, nylon 6/69 and PHBH) and material fractions (leachables, pure polymer and plastic (i.e., leachables + polymer)) of plastics during 21 days ($n = 3$, three technical replicates per biological triplicate as mean value, including standard deviation). The gating strategy is shown in Figure A7.

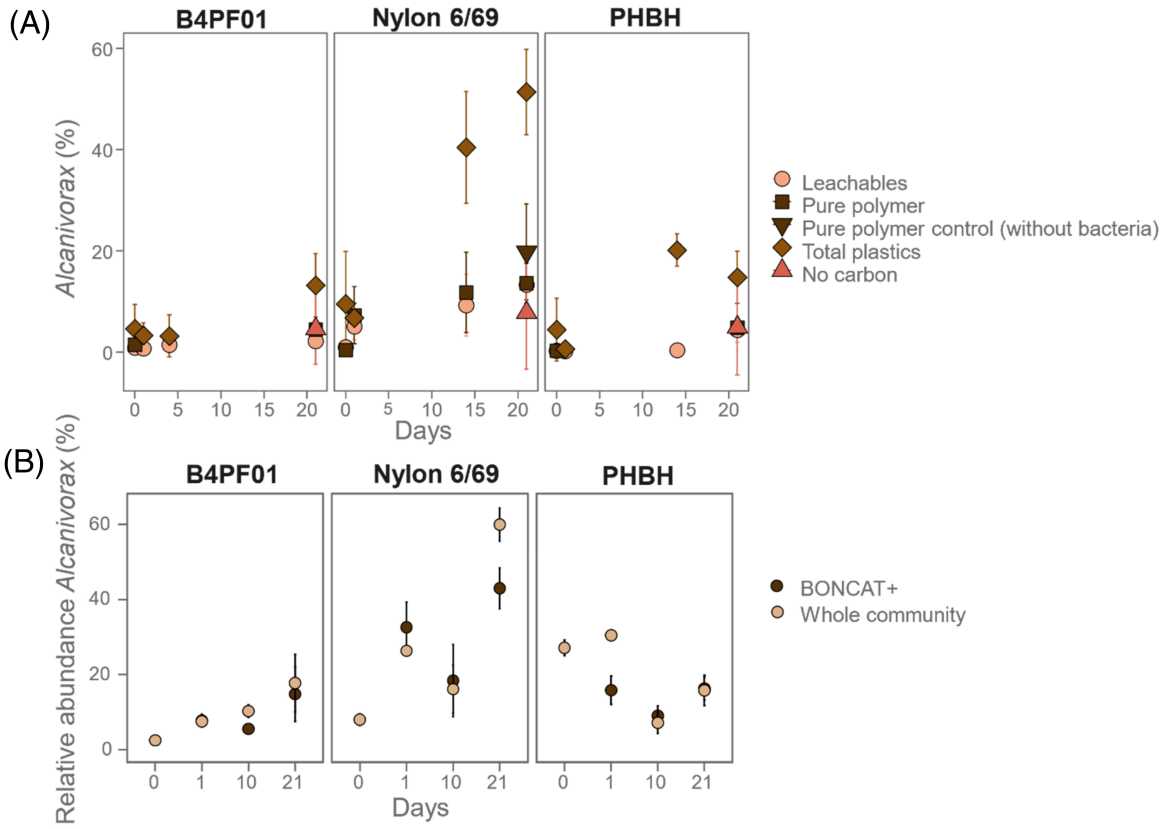

FIGURE 5 (A) The average percentage of cells, labelled with the *Alcanivorax* - FISH probe, compared to the total amount of cells, on different types (B4PF01, nylon 6/69 and PHBH) and material fractions (leachables, pure polymer and total plastics (i.e., leachables + polymer)) of plastics during 21 days ($n = 3$, three technical replicates per biological triplicate as mean value, including standard deviation). The gating strategy is shown in Figure A6. (B) The average relative abundance of the genus *Alcanivorax* (based on ASVs) present in the whole community and the protein synthesizing (based on BONCAT-FACS) population determined by 16S rRNA gene amplicon sequencing ($n = 3$) of the incubations with the total plastics fraction of different types (B4PF01, nylon 6/69 and PHBH) of plastics.

Activity of *Alcanivorax* species in a plastic-enriched community

To assess the relative abundance of *Alcanivorax* in the communities growing on different plastic types and material fractions, three complementary techniques, fluorescent in situ hybridisation in combination with flow cytometry (FISH), bioorthogonal non-canonical amino acid tagging in combination with cell sorting (BONCAT-FACS) followed by 16S rRNA gene amplicon sequencing and standard 16S rRNA gene amplicon sequencing, were used.

The *Alcanivorax*-FISH probe labelled cells significantly increased in abundance between Day 0 and Day 21 (from 4.6% ± 4.8% to 13.2% ± 6.3% for B4PF01 (Wilcoxon test, $p = 0.005$), from 9.5% ± 10.4% to 51.4% ± 8.4% for nylon 6/69 (Wilcoxon test, $p < 0.001$) and from 4.5% ± 6.2% to 14.8% ± 5.2% for PHBH (Wilcoxon test, $p = 0.002$)) in the incubation with the total plastics, as well as for leachable (Wilcoxon test, $p < 0.001$ for B4PF01, nylon 6/9 and PHBH) and pure polymer fractions (Wilcoxon test, $p < 0.001$ for B4PF01, nylon 6/9 and PHBH) (Figure 5A).

The relative abundance of *Alcanivorax*-FISH data on Day 21 is similar to the results from 16S rRNA gene amplicon sequencing data. The whole community has a relative abundance of *Alcanivorax* of 17.9% ± 7.7% for B4PF01, 62.7% ± 5.5% for nylon 6/69 and 16.0% ± 4.0% for PHBH, whereas the relative abundance of *Alcanivorax* in the protein synthesizing fraction of the population, using BONCAT-FACS is 14.8% ± 7.3% for B4PF01, 42.96 ± 5.43% for nylon 6/69 and 16.3% ± 3.0% for PHBH (Figure 5B).

The phenotypic diversity of the communities including the *Alcanivorax*-probe labelled cells on the different types and material fractions of plastics was investigated. The principal coordinate analysis (PCoA) of the beta-diversity of the FISH data shows phenotypic uniformity for the leachable and pure polymer fraction of all plastic types at the start of the experiment compared to the total plastics (Figure 6). After 21 days of incubation, the phenotypic fingerprint changed and less variance is explained by the first two axes. Within each material fraction, the beta diversity differentiates strongly, except for the B4PF01 leachables. On the other hand, permutational multivariate analysis of variance using distance matrices resulted in significant differences ($p < 0.001$) between each material fraction per plastic type.

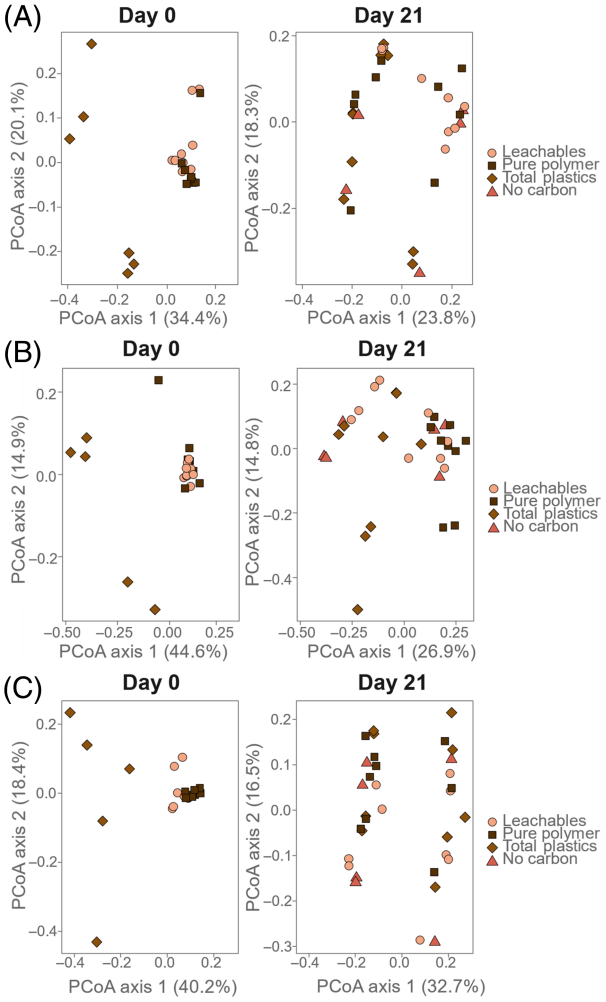

FIGURE 6 PCoA of the Bray–Curtis dissimilarity matrix of the FISH-data, showing beta-diversity of material fractions of (A) B4PF01, (B) nylon 6/69 and (C) PHBH ($n = 3$, three technical replicates per biological triplicate as mean value, including standard deviation). Minimal cell count cut-off = 500 cells (day 0); minimal cell count cut-off = 2000 cells (day 21).

Alcanivorax ASV behaviour in the plastic-enriched community

The different amplicon sequencing variants (ASV), classified as *Alcanivorax*, were investigated separately, as they indicate variation within the short sequences, which might be related to different *Alcanivorax* species. The most abundant ASVs present in the communities growing on the total plastics are ASV4, ASV5 and ASV6 (Figure 7). By placing the short sequences in a reference tree with type strains from EZBioCloud, they show the closest relatedness to *Alloalcanivorax mobilis* MT13131 (ASV4), *Alcanivorax* DS989915_s DG881 (ASV5) and *Alcanivorax borkumensis* SK2 (ASV6) (Figure A3). While ASV4 is mainly present in the B4PF01 and PHBH enrichment, ASV5 emerges in the nylon 6/69 and, to a much lesser extent, the PHBH enrichment. ASV6 is mainly present in B4PF01 and nylon 6/69 enrichment. The abundance and ratio of the ASVs are dynamic over time. While the relative abundance of the ASVs generally increases for B4PF01 and

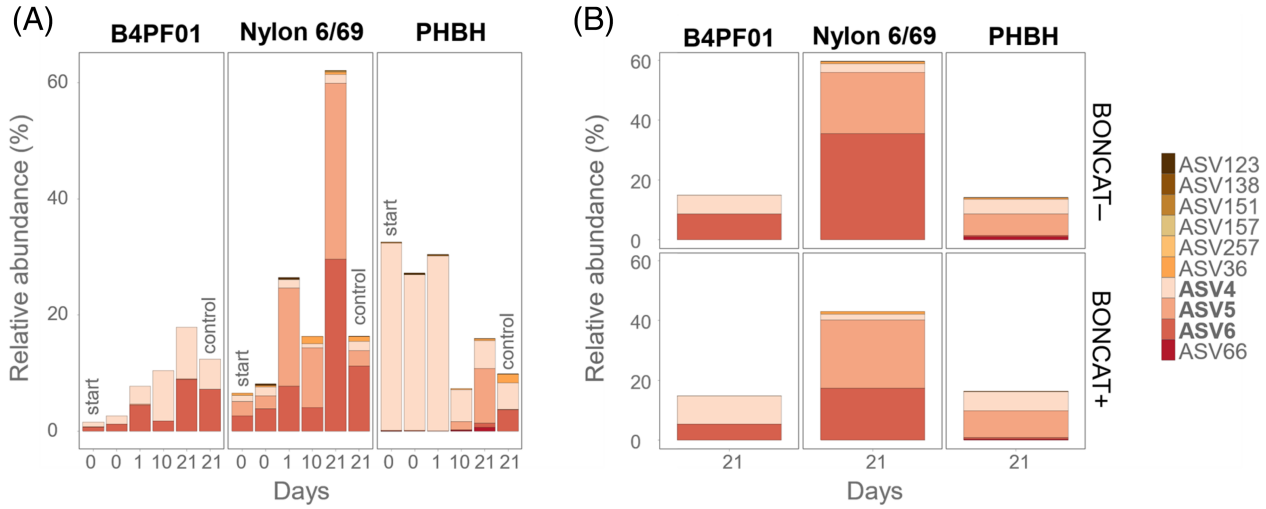

FIGURE 7 Relative abundance of the 10 most abundant ASVs classified as *Alcanivorax* within the microbial community during 21 days of incubation with the total plastics. The whole community (A), BONCAT+ and BONCAT-FACS sorted population (B) are shown. The complete community composition is given in Figure A4. *'start' is the inoculum, and 'control' is the incubation without plastics*.

nylon 6/69, it decreases in relative abundance in the PHBH enrichment over time, especially ASV4. Compared to the control without carbon, B4PF01 has a similar relative abundance (9.4% vs. 5.2% for ASV4 and 5.4% vs. 7.2% for ASV6, sample and controls, respectively). Nylon 6/69 has a much higher relative abundance of ASV5 and ASV6 compared to the control (30.4% vs. 2.7% for ASV5 and 29.6% vs. 11.2% for ASV6, sample and controls, respectively), and PHBH even has a different ASV composition. Comparing the BONCAT+ and BONCAT− populations (i.e., cells that actively synthesize proteins and cells that do not) at Day 21, the ASVs are more or less evenly distributed in the BONCAT− and BONCAT+ populations for all plastic types, except ASV6 in the nylon 6/69 community that has a twice higher BONCAT− relative abundance (Figure 7B).

Isolation of *Alcanivorax* species from plastic-enriched communities

An isolation campaign of the plastic-enriched communities was set up to obtain pure *Alcanivorax* strains. BLAST classification by EZBioCloud resulted in two different species: *Alcanivorax* sp. DG881 and *Alcanivorax borkumensis* (Table 5). The two *Alcanivorax* species closest related to *Alcanivorax* sp. DG881 and *A. borkumensis* originated from, respectively, plastics enrichments with a trickling filter with B4PF01 as carrier material and a flask enrichment with nylon 6/69 (Figure A1). This result correlates with the ASVs found in the corresponding incubations (Figure 7 and Figure A4).

TABLE 2 Isolated strains closest to the EZBioCloud database and corresponding seawater plastic enrichment.

Closest hit (% similarity)	Enrichment	Name used in this study
Alcanivorax sp. DG881 (100%)	Trickling Filter	*A.* DG881-like isolate
Alcanivorax borkumensis (98.93%)	Nylon 6/69 enrichment	*A. borkumensis*-like isolate

Growth and activity of axenic Alcanivorax species on plastic

The two *Alcanivorax* species were grown as axenic cultures on the total plastics fraction, in a similar setup to the enriched communities. The carrying capacity is different for the different plastic types, with the lowest carrying capacity for the *A.* DG881-like isolate on B4PF01 and the *A. borkumensis*-like isolate on nylon 6/69 (Table 6). Remarkably, the condition without carbon reaches similar cell concentrations as the condition with the biodegradable PHBH, confirmed by a similar carrying capacity (*A. borkumensis*-like isolate). The maximum growth rate is the highest for nylon 6/69 (*A.* DG881-like isolate) and PHBH (*A. borkumensis*-like isolate) (Figure 8).

Dissolved organic carbon (DOC) measures biodegradation

To give insight into the biodegradation of the total plastic, pure polymer and leachable fraction, DOC was

TABLE 3 Maximum growth rate and carrying capacity of isolates determined by the four-parametric logistic growth model.

	Growth rate (day^{-1})				Carrying capacity (cells/mL)			
	B4PF01	Nylon 6/69	PHBH	Control	B4PF01	Nylon 6/69	PHBH	Control
A. DG881-like isolate	0.229	1.473	0.185	NA[a]	1.9×10^6	3.3×10^6	9.6×10^6	NA[a]
A. borkumensis-like isolate	0.138	0.304	0.583	0.304	2.9×10^6	2.6×10^6	5.1×10^6	5.3×10^6

[a]Erroneous value was acquired for these data points (Sprouffske, 2020).

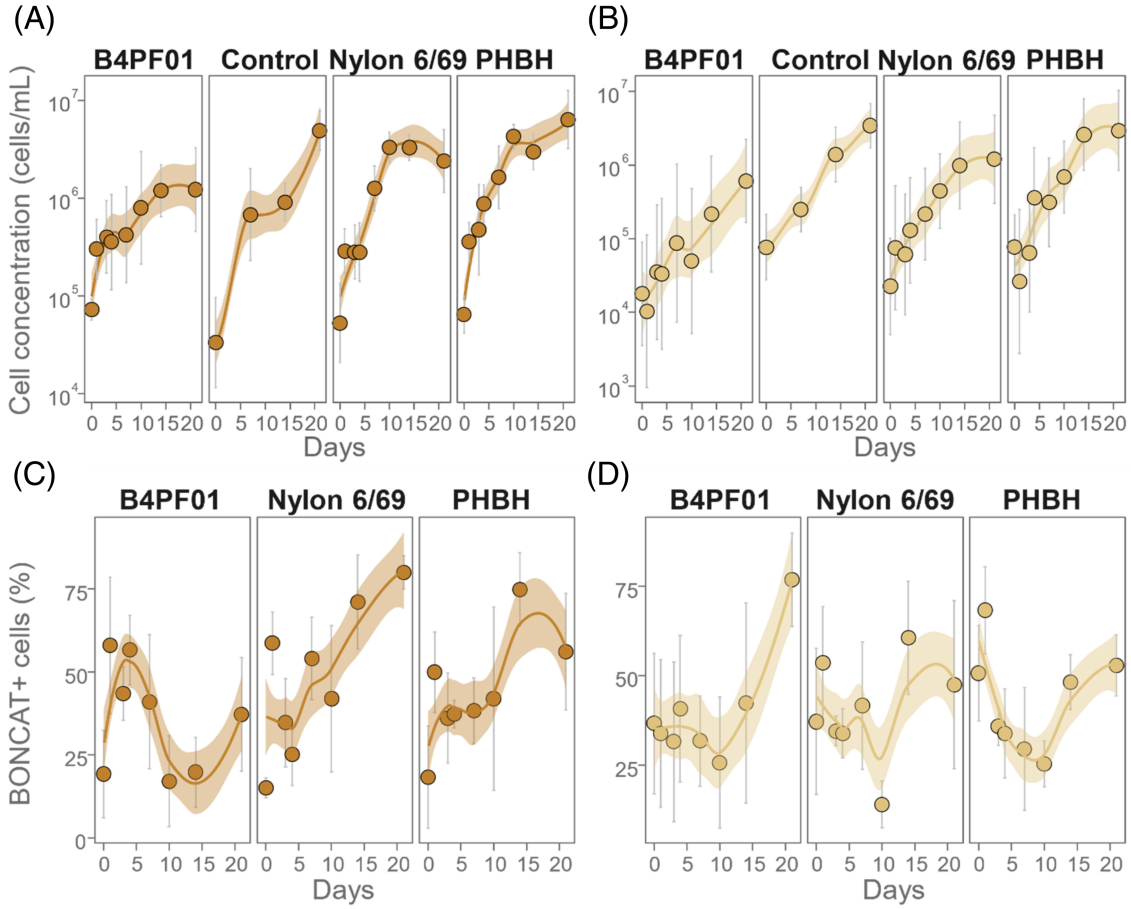

FIGURE 8 Cell growth of *A.* DG881-like isolate (A) and *A. borkumensis*-like isolate (B) on the total plastics fraction of different types of plastic ($n = 3$, three technical replicates per biological triplicate, including standard deviation). Control indicates the condition without (plastic) carbon source. (C, D) Percentage of BONCAT+ cells within the monoculture of *A. DG881-like* isolate and *A.* borkumensis-*like* isolate, indicating protein synthesis, grown on different types of plastics, measured with BONCAT ($n = 3$, three technical replicates per biological triplicate, standard deviation). The smoothing method used was loess, with a standard error given at the 0.95 confidence level. The gating strategy is shown in Figures A5 and A7.

measured. The concentration of leachables measured at the start was 434 μg/L ppb, 416 μg/L and 467 μg/L for B4PF01, nylon 6/69 and PHBH, respectively. After subtracting the DOC from the medium, it was calculated that the plastics B4PF01, nylon 6/69 and PHBH leached 273, 308 and 328 μg/L DOC, respectively, over 11 days of sterile incubation. For both B4PF01 and nylon 6/69, the DOC concentrations over the microbial incubation period of 21 days decreased, with a concentration of 186 μg/L for B4PF01 and 933 μg/L for nylon 6/69. Similarly, the DOC in the pure polymer incubations decreased during the 21 days in total 308 μg/L and 807 μg/L for B4PF01 and nylon 6/69, respectively. For PHBH, the opposite was noted, namely an increase in DOC for both leachables and pure polymer towards 450 and 1080 μg/L, respectively (Figure 9).

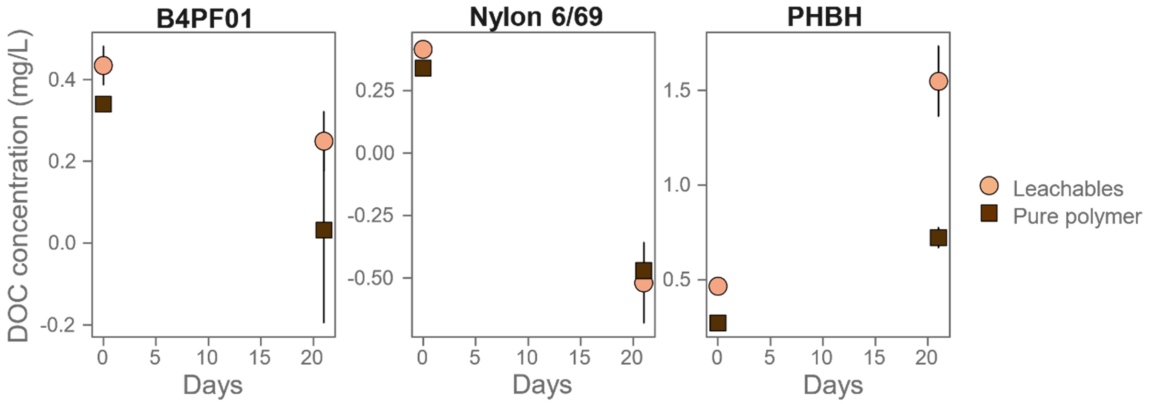

FIGURE 9 Dissolved Organic Carbon (DOC) present during incubation of both leachables and pure polymer as carbon source with the B4PF01-, nylon 6/69- and PHBH-enriched community. Values were subtracted from the values from the control samples ($n = 3$, four technical replicates per biological triplicate, standard deviation shown).

DISCUSSION

Quantifying the abundance of *Alcanivorax* in plastic communities using three methods

The average relative abundance of *Alcanivorax* growing in plastic communities was calculated using three complementary methods: fluorescent in situ hybridisation (FISH), bioorthogonal non-canonical amino acid tagging in combination with cell sorting followed by 16S rRNA gene amplicon sequencing (BONCAT-FACS) and standard 16S rRNA gene amplicon sequencing (Figure 5). Combining these three techniques allows us to obtain more insight into the role of *Alcanivorax* in terms of relative abundance in plastic-enriched communities (Table 7). Comparing the percentages of *Alcanivorax* at the start of the experiment on B4PF01 and nylon 6/69, FISH served as a representative alternative for standard 16S rRNA gene amplicon sequencing, indicating mainly active bacteria are present. However, for PHBH, a relative abundance difference of 23% using both techniques was observed, which could be caused by a high abundance of inactive (Karner & Fuhrman, 1997) or dead *Alcanivorax* (Li et al., 2017). When focussing on the percentages of *Alcanivorax* after 21 days of growth on B4PF01 and PHBH, FISH served as a representative alternative for both BONCAT-FACS+ and BONCAT-FACS− in combination with 16S rRNA gene amplicon sequencing and standard 16S rRNA gene amplicon sequencing. Zooming in on the BONCAT-FACS results, similar percentages of protein synthesizing and non-synthesizing *Alcanivorax* were observed, suggesting this genus was stagnantly present in plastic communities around 15% (B4PF01 and PHBH). On the other hand, the percentage of *Alcanivorax* on nylon 6/69 tends to decrease at 21 days. More specifically, the fraction of protein synthesizing, i.e., BONCAT-FACS+, *Alcanivorax* was around 17% lower than BONCAT-FACS− *Alcanivorax*. Additionally, the relative abundance by 16S rRNA gene amplicon sequencing of *Alcanivorax* on nylon 6/69 is 11% higher than the FISH result at day 21, whereas this difference was not observed at day 0. Using these different measurements enables us to quantify how the population is divided into protein synthesizing and non-synthesizing cells and cells with high and low RNA content, and hint towards functionality.

Material fractions give insights into early biofilm formation by *Alcanivorax*

Early biofilm formation (10 days) on plastics is reported to be dominated by *Gammaproteobacteria* such as *Alcanivoracaceae* (Odobel et al., 2021). *Alcanivorax* is furthermore known for biofilm formation in the context of oil dispersion and biodegradation (Omarova et al., 2019) and utilizes different morphologies (thick biofilm phenotype versus a thin dendritic phenotype) to optimize oil consumption (Prasad et al., 2022). This suggests that the biofilm has a dual functionality. On the one hand, it is produced to optimize oil degradation (through adsorption to the oil–water interface), and on the other hand for attachment (increasing growth rate). For the three different plastics, B4PF01, nylon 6/69 and PHBH, the highest cell concentrations were observed for the total plastics (Figure 2). This could indicate suboptimal conditions when microbial populations grow on leachable or pure polymer, suggesting the attachment of the cells on total plastics leads to the utilization of the easily available carbon source (leaching compounds). It might be probable that certain degradative enzymes are only induced upon biofilm formation, leading to enhanced biodegradation when the cells are attached (Pete, 2022). The effect of attachment could be easily investigated by adding non-plastic particles to the leachable incubation and observing the microbial

TABLE 4 Relative abundances of *Alcanivorax* in communities growing on the total plastics fractions of three different plastics, after 0 and 21 days of incubation, determined using three complementary methods.

	FISH			**BONCAT (+ and −)-FACS combined with 16S rRNA gene amplicon sequencing**			**16S rRNA gene amplicon sequencing**		
	Combined with flow cytometry, indicating a relative abundance of *Alcanivorax* in the total plastics community with minimal ribosomal content.			Indicating the relative abundance of *Alcanivorax* in the total plastics community that is actively synthesizing proteins.			Indicating the relative abundance of *Alcanivorax* in the total plastics community.		
	B4PF01	Nylon 6/69	PHBH	B4PF01	Nylon 6/69	PHBH	B4PF01	Nylon 6/69	PHBH
Day 0	4.6% ± 4.8%	9.5% ± 10.4%	4.5% ± 6.2%	-	-	-	2.7% ± 0.3%	8.2% ± 1.5%	27.2% ± 2.1%
Day 21	13.2% ± 6.3%	51.4% ± 8.4%	14.8% ± 5.2%	14.8% ± 7.3% (+) 14.9% ± 6.0% (−)	42.9% ± 5.4% (+) 59.6% ± 6.1% (−)	16.3% ± 3.0% (+) 14.0% ± 3.0% (−)	17.9% ± 7.7%	62.7% ± 5.5%	16.0% ± 4.0%

growth and degradation, as has been performed similarly for hexadecane degradation (Pete, 2022). The plastics in this study, and thus also the leachables, did not contain additives. However, the lower cell concentrations on the leachable fraction could be explained by its toxicity to the cells.

The differences in growth and activity on the material fractions are somewhat reflected in the PCoA ordination of the diversity of the phenotypic fingerprints using the FISH data (Figure 6). On the other hand, the permutational multivariate analysis of variance resulted in significant differences between each material fraction per plastic type. Communities tend to evolve from the initially inoculated planktonic culture to adapt to a sessile or planktonic lifestyle in media with plastics (Rummel et al., 2021). Sessile lifestyles include small bacterial aggregates as well as biofilms, and both have been reported to have similar phenotypes (Sauer et al., 2022). Incubations without additional carbon sources or growing on leachables would therefore be expected to be phenotypically differentiated from the incubations with pure polymer or total plastics fractions (Kragh et al., 2023). Nevertheless, the incomplete removal of biofilm on total plastics or pure polymer could still cause some bias in the obtained data (Rose et al., 2020), possibly explaining why the ordination did not pick up material fractions as an explanation for variation. Moreover, shifts in relative abundances due to the different material fractions can cause phenotypic fingerprints to change (Focardi et al., 2022; Props et al., 2016).

The differences in *Alcanivorax* abundances on the different types of (total) plastics might be linked to the difference in substrate hydrophobicity during early colonization (Ogonowski et al., 2018; Wright, Bosch, et al., 2021). However, substrate specificity is debatable and might vary over time, as early biofilm formation has also been reported to be non-substrate specific and the surface properties of polymer materials can change through weathering (Schefer et al., 2023).

Dissolved organic carbon as an indication for leachable biodegradation

The plastics B4PF01, nylon 6/69 and PHBH leached 0.0273%, 0.0308% and 0.0328% of the total plastic weight (in sterile conditions). This is only originating from residual monomeric and oligomeric compounds as no plastic additives were present. The leached DOC consists of building block molecules that failed to polymerize and remain as oligomers and monomers in the plastic matrix. For nylon 6/69, the building blocks ε-caprolactam and hexamethylenediamine have been reported as biodegradable (Klaeger et al., 2019; Tiso et al., 2022). The building blocks of PHBH, a known biopolymer that is biodegradable in seawater, are also

TABLE 5 Overview of sampling time points of the communities regarding different molecular techniques, accompanying sampling time points for Figures 2, 4 and 5.

		Flow cytometry			BONCAT			FISH			
	Day	L	PP	TP	L	PP	TP	L	PP	TP	16S rRNA sequencing
B4PF01	0	x	x	x	x	x	x	x	x	x	C
	1	x		x	x		x	x		x	C, B+
	4	x		x	x		x	x		x	
	10										C, B+
	14										
	21	x	x	x	x	x	x	x	x	x	C, B+, B−
Nylon 6/69	0	x	x	x	x	x	x	x	x	x	C
	1	x		x	x	x	x	x		x	C, B+
	4						x				
	10										C, B+
	14	x		x	x	x	x	x	x	x	
	21	x	x	x	x	x	x	x	x	x	C, B+, B−
PHBH	0	x	x	x	x	x	x	x	x	x	C
	1	x		x	x		x	x		x	C, B+
	4						x				
	10										C, B+
	14	x		x	x		x	x		x	
	21	x	x	x	x	x	x	x	x	x	C, B+, B−
Controls	0	LC, PPC (only PA 6/69)									
	21	NC, LC, PPC, TPC			NC			NC			

Note: Both the enriched communities with different material fractions (leachables (L), pure polymer (PP), total plastics (TP)) and controls (abiotic fraction containing leachables (LC), pure polymer (PPC) or total plastics (TPC) and biotic fraction without carbon (NC)) are indicated per day. The 16S rRNA gene amplicon sequencing was performed on the whole community (C) and after cell sorting of the BONCAT− (B−) and BONCAT+ cells (B+). Sampling time points and analyses were based on the growth phases (starting point, exponential phase and stationary phase) of the original plastic enrichments.

TABLE 6 Composition of 2.025 μL click-it dye mix for bio-orthogonal non-canonical amino acid tagging (BONCAT).

Click-it dye mix (2.025 μL)	
20 mM $CuSO_4$ (in Milli-Q™, 0.22 μm filter sterilized)	0.625 μL
50 mM THTPA (in Milli-Q™, 0.22 μm filter sterilized, Click Chemistry Tools, USA)	1.250 μL
Azide dye	0.150 μL
Alexa Fluor™ 647 Azide (AF647) (0.5 mM or 1 mM, in 0.22 μm-filtered dimethyl sulfoxide, Invitrogen, USA)	

TABLE 7 Composition of hybridization and washing buffer for fluorescence in situ hybridization (FISH), for both 20% stringency and 10 mL.

Hybridization buffer (10 mL) 20%		Washing buffer (10 mL) 20%	
5 M NaCl (autoclaved)	1800 μL	5 M NaCl (autoclaved)	430 μL
0.5 M Tris/HCl, pH 8 (autoclaved)	400 μL	0.5 M Tris/HCl, pH 8 (autoclaved)	400 μL
Formamide (Sigma-Aldrich™, USA)	2000 μL	0.5 M EDTA (di-sodium salt)	
pH 8.0 (autoclaved)	100 μL		
10% (wt/vol) SDS (0.22 μm filter sterilized)	20 μL	10% (wt/vol) SDS (0.22 μm filter sterilized)	10 μL
Milli-Q™ (0.22 μm filter sterilized)	5800 μL	Milli-Q™ (0.22 μm filter sterilized)	9060 μL

biodegradable (Eraslan et al., 2022; Wang et al., 2018). Namely, its major unit (89%–99%), 3-hydroxybutyric acid, is an intermediate in fatty acid metabolism and its minor unit (1%–11%), 3-hydroxyhexanoic acid, a primary metabolite (*Human Metabolome Database: Showing metabocard for ®-3-Hydroxyhexanoic acid (HMDB0010718)*, Human Metabolome Database, 2008; EFSA Panel on Food Contact Materials, Enzymes, Flavourings and Processing Aids (CEF), 2016). No biodegradability data is available for the novel B4PF01 plastic. For every plastic type, the cell concentrations increased in the leachable incubations. The cell concentration at Day 21 was significantly lower than for the total plastics incubations, suggesting that leachables impair growth as reported in other

studies (Costa et al., 2023; Focardi et al., 2022; Tetu et al., 2019) and/or the importance of a growth substrate and bacterial attachment for biodegradation.

Combining the cell growth data with the results from the DOC measurements of the leachables, it is observed that the DOC decreases during the incubation for B4PF01 and nylon 6/69 (Figure 9). However, the decrease in DOC for the leachables is smaller or of similar magnitude as in the pure polymer incubations. The decrease could indicate that the labile part of the DOC from the medium (403 μg/L) is additionally used as a carbon source. Our results confirm heterotrophic growth in the pure medium when no carbon source was added for both the microbial communities and the isolates (Figures 2 and 8). More information on microbial growth in lower carbon concentrations is found in the Appendix B. Furthermore, the initial concentration of leachable DOC alone does not contain sufficient carbon to sustain the observed growth of 2.6×10^6 cells/mL for B4PF01, 1.6×10^6 cells/mL for nylon 6/69 leachables, assuming that the carbon requirement for microbial growth can be estimated as 1 mg/L DOC per 10^6 cells/mL and only 60% of the leached DOC is available for microbial utilization (Romera-Castillo et al., 2022). Part of the decrease in DOC can also be attributed to the pure polymer that re-adsorbs DOC from the medium (Romera-Castillo et al., 2018), explaining why the DOC decreased to a greater extent in the pure polymer incubations compared to the leachables. Remarkably, the DOC of the PHBH leachables increases during the incubation period. As this opposes the conservation of mass, we assume the DOC measurement is erroneous.

Nylon, a biodegradable plastic or not?

The degradability of nylon is debated, which can be partially attributed to the different grades of nylon that exist. For example, nylon 11 is reported as a non-biodegradable polymer, while nylon 4 is biodegradable (Tokiwa et al., 2009). This is most probably due to the difference in hydrophobicity (Min et al., 2020). Furthermore, the degradation test conditions are important. It has been reported that nylon 6 is used as a carbon and nitrogen source by landfill isolates (Oulidi et al., 2022; Tiwari et al., 2024) and marine bacteria in seawater at 35°C (Sudhakar et al., 2007), while in seawater at 25°C, nylon 6 was not biodegraded unless a UV pretreatment was used (An et al., 2023). A different issue of nylon 6 biodegradation has been addressed by Klaeger et al. (2019). They describe the misinterpretation of the biodegradation of nylon 6 by measuring the biodegradation of dissolved organic carbon from leached residual monomeric and oligomeric content instead of plastic. Nylon 6 differs from nylon 6/69 in monomer composition as nylon 6 is a homopolymer of caprolactam and nylon 6/69 is a copolymer made from caprolactam and hexamethylenediamine. However, it was observed that microbial growth on the total plastics fraction is higher compared to the other fractions combined (Figure 3). Interestingly, the nylon-enriched community control without carbon has a higher cell density at Day 21 compared to the leachables and the pure polymer (Figure 2). Both results challenge the assumption that nylon biodegradation might be wrongly concluded from leachate biodegradation (Klaeger et al., 2019). This statement is strengthened by the DOC concentration of the nylon 6/69 leachables that decreases a similar amount for the samples as the abiotic controls (Figure 9).

When zooming in on *Alcanivorax*, this genus has a very high abundance of around 60% in both the FISH and the BONCAT-FACS 16S rRNA gene amplicon sequencing data, compared to its abundance in the other plastic incubations. Following the degradation mechanisms of nylon 6,6 (a copolymer made from hexamethylenediamine and adipic acid) proposed by Tiwari et al. (2022, 2024), the release of hydrocarbons in the degradation process could explain the proliferation of *Alcanivorax* sp. (Péquin et al., 2022). The success of *Alcanivorax* to increase in abundance from undetectable in pristine water to 60%–70% of the microbial community in oil-polluted seawater (with most efficient degradation of branched, saturated alkanes) compared to other hydrocarbonoclastic genera has been reported before (Cafaro et al., 2013; Hara et al., 2003). The extracellular enzymes for nylon 6,6 degradation, laccases and peroxidases are encoded in different *Alcanivorax* species, amongst others, *A. borkumensis* and *A.* sp. DG881 encodes for peroxidases (*GSHPx - Glutathione peroxidase - Alcanivorax borkumensis (strain ATCC 700651 / DSM 11573 / NCIMB 13689 / SK2)* | *UniProtKB* | *UniProt*, GSHPx, n.d.; *(taxonomy_id:236097) peroxidase in UniProtKB search (15)* | *UniProt*), (Taxonomy ID 236097, n.d.). Furthermore, some *Alcanivorax* sp. are capable of degrading caprolactam (*alk1* gene); amongst others, *A. borkumensis*. In conclusion, this study strengthens the assumption that nylon 6/69 can be biodegraded in an enriched seawater community, favouring *Alcanivorax* and sustaining the growth of *Alcanivorax* in axenic cultures.

Alcanivorax on plastics, as both axenic culture and part of the community

The isolates used in our study were closest related to *Alcanivorax* sp. DG881 (*A.* DG881-like isolate) and *Alcanivorax borkumensis* SK2 (*A. borkumensis*-like isolate) according to EZBioCloud. Using the same database, the three most abundant ASVs were identified as *Alloalcanivorax mobilis* MT13131 (ASV4), *Alcanivorax*

sp. DG881 (ASV5) and *Alcanivorax borkumensis* SK2 (ASV6). By the evolutionary placement algorithm, the ASVs were placed in a phylogenetic tree, and identically classified (Figure A3). The ASVs, only consisting of the V3-V4 region of the 16S rRNA, however, were differently placed in the phylogenetic tree compared to the BLAST identification. These short sequences might not be optimal for correctly classifying the closely related *Alcanivorax* sp. DG881 and *Alcanivorax borkumensis* SK2 (Bukin et al., 2019; Dede et al., 2023; Heather & Chain, 2016). By making a multiple sequence alignment, the short reads were mapped on the full 16S sequences. It was indicated that most of the sequence differences were located outside the V3–V4 region (4 vs 25 nt difference).

The three plastics used in this study have different profiles of *Alcanivorax* ASVs. The incubation with PHBH is mainly comprised by ASV4 (*Alloalcanivorax mobilis* MT13131), while B4PF01 has both ASV4 (*A. mobilis* MT13131) and ASV6 (*Alcanivorax borkumensis* SK2) and nylon 6/69 has both ASV5 (*Alcanivorax* sp. DG881) and ASV6 (*A. borkumensis* SK2) (Figure 7). This can be linked to the properties of the plastic, such as the presence of ester bonds in PHBH and amide bonds in B4PF01 and nylon 6/69. Consequently, the performance of *A*. DG881-like isolate on nylon 6/69 and *A. borkumensis*-like isolate on B4PF01 are reflected in the community composition. *A*. DG881-like isolate has a higher protein synthesis, growth rate and carrying capacity on nylon 6/69 compared to *A. borkumensis*-like isolate (Figure 8). This can be related to the relative abundance of ASV 5 (*Alcanivorax* sp. DG881) that increases in abundance to 30% ± 8% (whole community) and 22.8% ± 8% (BONCAT+) at Day 21 (Figure 7A). Furthermore, the population of BONCAT+ cells has a higher relative abundance of ASV5 than ASV6 (Figure 7B). Similarly, *A. borkumensis*-like isolate has a higher protein synthesis and carrying capacity on B4PF01, which is reflected in the relative abundance by 16S rRNA gene amplicon sequencing (Figure 8). In conclusion, the *Alcanivorax* isolates that were found in the plastic-enriched communities can grow and actively synthesize proteins when they are part of a community and as axenic culture, on plastic. Furthermore, the results suggest a plastic-specific differentiation and distribution of the *Alcanivorax* species that could be linked to a substrate-specific functional diversity (Miao et al., 2021).

CONCLUSION

This study aimed to contribute to the understanding of plastic-enriched communities' behaviour by investigating three distinct fractions (leachables, pure polymer and total plastics) and three different types of plastics (novel plastics B4PF01, nylon 6/69 and PHBH). Herein, we focussed on the genus *Alcanivorax* as part of the community as well as two axenic cultures, originally isolated from these communities. From our study, it can be concluded that *Alcanivorax* exhibits a preference for the (total) plastic over leachables and pure polymer fraction alone when growing in a community setting. Remarkably, *Alcanivorax* maintains detectable relative abundances when no carbon source is present. Enriched *Alcanivorax* communities and axenic cultures grow to comparable cell concentrations in the absence of a carbon source, suggesting an efficient use of limited resources. Furthermore, *Alcanivorax* species seems to have adapted to chemically different polymers and a different spectrum of ASVs was noted for different types of plastics. The species specialization is confirmed by *Alcanivorax's* high cell concentrations and protein synthesis in axenic cultures. Additionally, our results suggest that nylon 6/69 may be biodegraded by the community, particularly favouring *Alcanivorax borkumensis*, as evidenced by its dominant relative abundance in the community and decreasing DOC concentration. This collective evidence strengthens the hypothesis that *Alcanivorax* plays a main role in the biodegradation of certain plastic types within enriched communities.

AUTHOR CONTRIBUTIONS

Valérie Mattelin: Conceptualization; methodology; investigation; writing – original draft; writing – review and editing. **Astrid Rombouts:** Conceptualization; methodology; investigation; writing – original draft; writing – review and editing. **Josefien Van Landuyt:** Conceptualization; methodology; investigation. **Alberto Scoma:** Supervision. **Nico Boon:** Conceptualization; supervision; funding acquisition; project administration.

ACKNOWLEDGEMENTS

VM is funded by the Agentschap Innoveren en Ondernemen (VLAIO, Belgium) and B4Plastics (Dilsen-Stokkem, Belgium) via a Baekeland PhD fellowship (grant number HBC.2019.2622). AR is funded by a PhD fellowship strategic basic research 1S24323N (FWO). JVL is funded by a Postdoctoral Fellowship Junior 1288224N (FWO). NB is funded by the research foundation BOF (Ghent University, Belgium) (BOF.BAS.2022.0014.01). The authors thank Thomas Pluym and Karel Folens for their critical review.

CONFLICT OF INTEREST STATEMENT

The authors declare no conflicts of interest.

DATA AVAILABILITY STATEMENT

The raw 16S rRNA amplicon data for this study can be found in the National Centre for Biotechnology Information (NCBI) database under BioProject PRJNA1093067: https://www.ncbi.nlm.nih.gov/bioproject/PRJNA1093067.

ORCID

Valérie Mattelin https://orcid.org/0000-0001-8202-5022

REFERENCES

An, Y., Kajiwara, T., Padermshoke, A., van Nguyen, T., Feng, S., Mokudai, H. et al. (2023) Environmental degradation of nylon, poly(ethylene terephthalate) (PET), and poly(vinylidene fluoride) (PVDF) fishing line fibers. *ACS Applied Polymer Materials*, 5(6), 4427–4436. Available from: https://doi.org/10.1021/acsapm.3c00552

Andersson, M.G.I., Catalán, N., Rahman, Z., Tranvik, L.J., & Lindström, E.S. (2018) Effects of sterilization on dissolved organic carbon (DOC) composition and bacterial utilization of DOC from lakes, *Aquatic Microbial Ecology*, 82(2), pp. 199–208. Available from: https://doi.org/10.3354/ame01890

Barbera, P., Kozlov, A.M., Czech, L., Morel, B., Darriba, D., Flouri, T. et al. (2019) EPA-ng: massively parallel evolutionary placement of genetic sequences. *Systematic Biology*, 68(2), 365–369. Available from: https://doi.org/10.1093/sysbio/syy054

Bos, R.P., Kaul, D., Zettler, E.R., Hoffman, J.M., Dupont, C.L., Amaral-Zettler, L.A. et al. (2023) Plastics select for distinct early colonizing microbial populations with reproducible traits across environmental gradients. *Environmental Microbiology*, 25(12), 2761–2775. Available from: https://doi.org/10.1111/1462-2920.16391

Bryant, J.A. et al. (2016) Diversity and activity of communities inhabiting plastic debris in the North Pacific gyre. *mSystems*, 1(3). Available from: https://doi.org/10.1128/msystems.00024-16

Buchanan, J.R. (2014) 3.13- decentralized wastewater treatment. In: S. Ahuja (Ed.) *Comprehensive water quality and purification*. Waltham: Elsevier, pp. 244–267. Available from: https://doi.org/10.1016/B978-0-12-382182-9.00050-5

Bukin, Y.S., Galachyants, Y.P., Morozov, I.V., Bukin, S.V., Zakharenko, A.S. & Zemskaya, T.I. (2019) The effect of 16S rRNA region choice on bacterial community metabarcoding results. *Scientific Data*, 6(1), 190007. Available from: https://doi.org/10.1038/sdata.2019.7

Cafaro, V., Izzo, V., Notomista, E. & di Donato, A. (2013) 14 - marine hydrocarbonoclastic bacteria. In: Trincone, A. (Ed.) *Marine enzymes for biocatalysis*. Sawston, CA: Woodhead Publishing (Woodhead Publishing Series in Biomedicine), pp. 373–402. Available from: https://doi.org/10.1533/9781908818355.3.373

Callahan, B.J., McMurdie, P.J., Rosen, M.J., Han, A.W., Johnson, A.J.A. & Holmes, S.P. (2016) DADA2: high-resolution sample inference from Illumina amplicon data. *Nature Methods*, 13(7), 581–583. Available from: https://doi.org/10.1038/nmeth.3869

Cao, Y., Zhang, B., Cai, Q., Zhu, Z., Liu, B., Dong, G. et al. (2022) Responses of *Alcanivorax* species to marine alkanes and polyhydroxybutyrate plastic pollution: importance of the ocean hydrocarbon cycles. *Environmental Pollution*, 313, 120177. Available from: https://doi.org/10.1016/j.envpol.2022.120177

Costa, J.P.d. et al. (2023) Plastic additives and microplastics as emerging contaminants: mechanisms and analytical assessment. *Trends in Analytical Chemistry*, 158, 116898. Available from: https://doi.org/10.1016/j.trac.2022.116898

Datta, M.S., Sliwerska, E., Gore, J., Polz, M.F. & Cordero, O.X. (2016) Microbial interactions lead to rapid micro-scale successions on model marine particles. *Nature Communications*, 7(11965). Available from: https://doi.org/10.1038/ncomms11965

De Tender, C. et al. (2017) Temporal dynamics of bacterial and fungal colonization on plastic debris in the North Sea. *Environmental Science & Technology*, 51(13), 7350–7360. Available from: https://doi.org/10.1021/acs.est.7b00697

De Tender, C.A. et al. (2015) Bacterial community profiling of plastic litter in the Belgian part of the North Sea. *Environmental Science & Technology*, 49(16), 9629–9638. Available from: https://doi.org/10.1021/acs.est.5b01093

Dede, B., Priest, T., Bach, W., Walter, M., Amann, R. & Meyerdierks, A. (2023) High abundance of hydrocarbon-degrading *Alcanivorax* in plumes of hydrothermally active volcanoes in the South Pacific Ocean. *The ISME Journal*, 17(4), 600–610. Available from: https://doi.org/10.1038/s41396-023-01366-4

Delacuvellerie, A., Cyriaque, V., Gobert, S., Benali, S. & Wattiez, R. (2019) The plastisphere in marine ecosystem hosts potential specific microbial degraders including *Alcanivorax borkumensis* as a key player for the low-density polyethylene degradation. *Journal of Hazardous Materials*, 380, 120899. Available from: https://doi.org/10.1016/j.jhazmat.2019.120899

Delacuvellerie, A., Géron, A., Gobert, S. & Wattiez, R. (2022) New insights into the functioning and structure of the PE and PP plastispheres from the Mediterranean Sea. *Environmental Pollution*, 295, 118678. Available from: https://doi.org/10.1016/j.envpol.2021.118678

Dey, S., Rout, A.K., Behera, B.K. & Ghosh, K. (2022) Plastisphere community assemblage of aquatic environment: plastic-microbe interaction, role in degradation and characterization technologies. *Environmental Microbiomes*, 17(1), 32. Available from: https://doi.org/10.1186/s40793-022-00430-4

Dixon, P. (2003) Computer program review VEGAN, a package of R functions for community ecology. *Journal of Vegetation Science*, 14(6), 927–930.

DSMZ GmbH. (2007) ONR7a medium.

Dussud, C. et al. (2018) Evidence of niche partitioning among bacteria living on plastics, organic particles and surrounding seawaters. *Environmental Pollution (Barking, Essex: 1987)*, 236, 807–816. Available from: https://doi.org/10.1016/j.envpol.2017.12.027

Dussud, C., Hudec, C., George, M., Fabre, P., Higgs, P., Bruzaud, S. et al. (2018) Colonization of non-biodegradable and biodegradable plastics by marine microorganisms. *Frontiers in Microbiology*, 9. Available from: https://doi.org/10.3389/fmicb.2018.01571 Accessed 5th January 2024.

Ebrahimi, A., Schwartzman, J. & Cordero, O.X. (2019) Cooperation and spatial self-organization determine rate and efficiency of particulate organic matter degradation in marine bacteria. *Proceedings of the National Academy of Sciences of the United States of America*, 116(46), 23309–23316. Available from: https://doi.org/10.1073/pnas.1908512116

EFSA Panel on Food Contact Materials, Enzymes, Flavourings and Processing Aids (CEF). (2016) SUPERSEDED: safety assessment of the substance poly((R)-3-hydroxybutyrate-co-(R)-3-hydroxyhexanoate) for use in food contact materials. *EFSA Journal*, 14(5), e04464. Available from: https://doi.org/10.2903/j.efsa.2016.4464

Eraslan, K., Aversa, C., Nofar, M., Barletta, M., Gisario, A., Salehiyan, R. et al. (2022) Poly(3-hydroxybutyrate-co-3-hydroxyhexanoate) (PHBH): synthesis, properties, and applications - a review. *European Polymer Journal*, 167, 111044. Available from: https://doi.org/10.1016/j.eurpolymj.2022.111044

Erni-Cassola, G., Wright, R.J., Gibson, M.I. & Christie-Oleza, J.A. (2020) Early colonization of weathered polyethylene by distinct bacteria in marine coastal seawater. *Microbial Ecology*, 79(3), 517–526. Available from: https://doi.org/10.1007/s00248-019-01424-5

Focardi, A., Moore, L.R., Raina, J.B., Seymour, J.R., Paulsen, I.T. & Tetu, S.G. (2022) Plastic leachates impair picophytoplankton and dramatically reshape the marine microbiome. *Microbiome*, 10(1), 179. Available from: https://doi.org/10.1186/s40168-022-01369-x

GSHPx. (n.d.) *Glutathione peroxidase - Alcanivorax borkumensis (strain ATCC 700651 / DSM 11573 / NCIMB 13689 / SK2)* | *UniProtKB* | *UniProt*. https://www.uniprot.org/uniprotkb/Q0VL62/entry Accessed 5th January 2024.

Hammes, F.A. & Egli, T. (2005) New method for Assimilable organic carbon determination using flow-cytometric enumeration and a natural microbial consortium as inoculum. *Environmental Science & Technology*, 39(9), 3289–3294. Available from: https://doi.org/10.1021/es048277c

Hara, A., Syutsubo, K. & Harayama, S. (2003) *Alcanivorax* which prevails in oil-contaminated seawater exhibits broad substrate specificity for alkane degradation. *Environmental Microbiology*, 5(9), 746–753. Available from: https://doi.org/10.1046/j.1468-2920.2003.00468.x

Heather, J.M. & Chain, B. (2016) The sequence of sequencers: the history of sequencing DNA. *Genomics*, 107(1), 1–8. Available from: https://doi.org/10.1016/j.ygeno.2015.11.003

Human Metabolome Database: Showing metabocard for (R)-3-Hydroxyhexanoic acid (HMDB0010718) (2008). Available at: https://hmdb.ca/metabolites/HMDB0010718 (Accessed 5th January 2024).

Jacquin, J., Cheng, J., Odobel, C., Pandin, C., Conan, P., Pujo-Pay, M. et al. (2019) Microbial ecotoxicology of marine plastic debris: a review on colonization and biodegradation by the "Plastisphere". *Frontiers in Microbiology*, 10. Available from: https://doi.org/10.3389/fmicb.2019.00865 Accessed 14th February 2023.

KANEKA. (n.d.) *Biodegradable Polymer Green Planet™* | *Kaneka*. https://www.kaneka.be/technology-products/kaneka-biodegradable-polymer-green-planettm Accessed 27th February 2024.

Karner, M. & Fuhrman, J.A. (1997) Determination of active marine Bacterioplankton: a comparison of universal 16S rRNA probes, autoradiography, and nucleoid staining. *Applied and Environmental Microbiology*, 63(4), 1208–1213. Available from: https://doi.org/10.1128/aem.63.4.1208-1213.1997

Kirstein, I.V., Wichels, A., Gullans, E., Krohne, G. & Gerdts, G. (2019) The Plastisphere – uncovering tightly attached plastic "specific" microorganisms. *PLoS One*, 14(4), e0215859. Available from: https://doi.org/10.1371/journal.pone.0215859

Klaeger, F., Tagg, A.S., Otto, S., Bienmüller, M., Sartorius, I. & Labrenz, M. (2019) Residual monomer content affects the interpretation of plastic degradation. *Scientific Reports*, 9(1), 2120. Available from: https://doi.org/10.1038/s41598-019-38685-6

Klindworth, A., Pruesse, E., Schweer, T., Peplies, J., Quast, C., Horn, M. et al. (2013) Evaluation of general 16S ribosomal RNA gene PCR primers for classical and next-generation sequencing-based diversity studies. *Nucleic Acids Research*, 41(1), e1. Available from: https://doi.org/10.1093/nar/gks808

Kragh, K.N., Tolker-Nielsen, T. & Lichtenberg, M. (2023) The non-attached biofilm aggregate. *Communications Biology*, 6(1), 1–13. Available from: https://doi.org/10.1038/s42003-023-05281-4

Lauro, F.M., McDougald, D., Thomas, T., Williams, T.J., Egan, S., Rice, S. et al. (2009) The genomic basis of trophic strategy in marine bacteria, *Proceedings of the National Academy of Sciences*, 106(37), pp. 15527–15533. Available from: https://doi.org/10.1073/pnas.0903507106

Letunic, I. & Bork, P. (2019) Interactive tree of life (iTOL) v4: recent updates and new developments. *Nucleic Acids Research*, 47(W1), 256–259. Available from: https://doi.org/10.1093/nar/gkz239

Li, R., Tun, H.M., Jahan, M., Zhang, Z., Kumar, A., Dilantha Fernando, W.G. et al. (2017) Comparison of DNA-, PMA-, and RNA-based 16S rRNA Illumina sequencing for detection of live bacteria in water. *Scientific Reports*, 7, 5752. Available from: https://doi.org/10.1038/s41598-017-02516-3

Mariën, Q., Candry, P., Hendriks, E., Carvajal-Arroyo, J.M. & Ganigué, R. (2022) Substrate loading and nutrient composition steer caproic acid production and biofilm aggregation in high-rate granular reactors. *Journal of Environmental Chemical Engineering*, 10(3), 107727. Available from: https://doi.org/10.1016/j.jece.2022.107727

McMurdie, P.J. & Holmes, S. (2013) Phyloseq: An R package for reproducible interactive analysis and graphics of microbiome census data. *PLoS One*, 8(4), 1–11. Available from: https://doi.org/10.1371/journal.pone.0061217

Miao, L., Yu, Y., Adyel, T.M., Wang, C., Liu, Z., Liu, S. et al. (2021) Distinct microbial metabolic activities of biofilms colonizing microplastics in three freshwater ecosystems. *Journal of Hazardous Materials*, 403, 123577. Available from: https://doi.org/10.1016/j.jhazmat.2020.123577

Min, K., Cuiffi, J.D. & Mathers, R.T. (2020) Ranking environmental degradation trends of plastic marine debris based on physical properties and molecular structure. *Nature Communications*, 11(1), 727. Available from: https://doi.org/10.1038/s41467-020-14538-z

Oberbeckmann, S. & Labrenz, M. (2020) Marine microbial assemblages on microplastics: diversity, adaptation, and role in degradation. *Annual Review of Marine Science*, 12(1), 209–232. Available from: https://doi.org/10.1146/annurev-marine-010419-010633

Odobel, C., Dussud, C., Philip, L., Derippe, G., Lauters, M., Eyheraguibel, B. et al. (2021) Bacterial abundance, diversity and activity during long-term colonization of non-biodegradable and biodegradable plastics in seawater. *Frontiers in Microbiology*, 12. Available from: https://doi.org/10.3389/fmicb.2021.734782 Accessed 21st November 2023.

Ogonowski, M., Motiei, A., Ininbergs, K., Hell, E., Gerdes, Z., Udekwu, K.I. et al. (2018) Evidence for selective bacterial community structuring on microplastics. *Environmental Microbiology*, 20(8), 2796–2808. Available from: https://doi.org/10.1111/1462-2920.14120

Omarova, M., Swientoniewski, L.T., Mkam Tsengam, I.K., Blake, D.A., John, V., McCormick, A. et al. (2019) Biofilm formation by hydrocarbon-degrading marine bacteria and its effects on oil dispersion. *ACS Sustainable Chemistry & Engineering*, 7(17), 14490–14499. Available from: https://doi.org/10.1021/acssuschemeng.9b01923

Oulidi, O., Nakkabi, A., Bouymajane, A., Elaraaj, I., Filali, F.R., Fahim, M. et al. (2022) 'Biodegradation of polyamide 6 by *Lysinibacillus* sp, *Alcaligene faecalis* and *Enterococcus faecalis*. *Cleaner Chemical Engineering*, 3, 100054. Available from: https://doi.org/10.1016/j.clce.2022.100054

Péquin, B., Cai, Q., Lee, K. & Greer, C.W. (2022) Natural attenuation of oil in marine environments: a review. *Marine Pollution Bulletin*, 176, 113464. Available from: https://doi.org/10.1016/j.marpolbul.2022.113464

Parker, D.S. Jacobs, T., Bower, E., Stowe, D.W., & Farmer, G. (1997) Maximizing trickling filter nitrification rates through biofilm control: research review and full scale application, *Water Science and Technology*, 36(1), pp. 255–262. Available from: https://doi.org/10.1016/S0273-1223(97)00332-6

Pete, A. (2022) 'Bioremediation of petroleum-based contaminants by alkane-degrading bacterium *Alcanivorax borkumensis*', *LSU Doctoral Dissertations* [Preprint].

Prévoteau, A., Kerckhof, F.M., Clauwaert, P. & Rabaey, K. (2021) Electrochemical and phylogenetic comparisons of oxygen-reducing electroautotrophic communities. *Biosensors and Bioelectronics*, 171, 1–20. Available from: https://doi.org/10.1016/j.bios.2020.112700

Prasad, M. et al. (2022) *Alcanivorax borkumensis* biofilms enhance oil degradation by interfacial tubulation. *bioRxiv*. Available from: https://doi.org/10.1101/2022.08.06.503017

Props, R., Monsieurs, P., Mysara, M., Clement, L. & Boon, N. (2016) Measuring the biodiversity of microbial communities by flow cytometry. *Methods in Ecology and Evolution*, 7(11), 1376–1385. Available from: https://doi.org/10.1111/2041-210X.12607

Quast, C., Pruesse, E., Yilmaz, P., Gerken, J., Schweer, T., Yarza, P. et al. (2013) The SILVA ribosomal RNA gene database project: improved data processing and web-based tools. *Nucleic Acids Research*, 41(D1), D590–D596. Available from: https://doi.org/10.1093/nar/gks1219

R Core Team (2020). *R: A language and environment for statistical computing*. R Foundation for Statistical Computing, Vienna, Austria. Available from: https://www.R-project.org/

Radwan, S.S., Khanafer, M.M. & Al-Awadhi, H.A. (2019) Ability of the so-called obligate hydrocarbonoclastic bacteria to utilize nonhydrocarbon substrates thus enhancing their activities despite their misleading name. *BMC Microbiology*, 19(1), 41. Available from: https://doi.org/10.1186/s12866-019-1406-x

Roager, L. & Sonnenschein, E.C. (2019) Bacterial candidates for colonization and degradation of marine plastic debris. *Environmental Science and Technology*, 53(20), 11636–11643. Available from: https://doi.org/10.1021/acs.est.9b02212

Romera-Castillo, C. et al. (2022) Aged plastic leaching of dissolved organic matter is two orders of magnitude higher than virgin plastic leading to a strong uplift in marine microbial activity. *Frontiers in Marine Science*, 9. Available from: https://doi.org/10.3389/fmars.2022.861557 Accessed 29th December 2023.

Romera-Castillo, C., Pinto, M., Langer, T.M., Álvarez-Salgado, X.A. & Herndl, G.J. (2018) Dissolved organic carbon leaching from plastics stimulates microbial activity in the ocean. *Nature Communications*, 9(1), 1430. Available from: https://doi.org/10.1038/s41467-018-03798-5

Rose, R.-S., Richardson, K.H., Latvanen, E.J., Hanson, C.A., Resmini, M. & Sanders, I.A. (2020) Microbial degradation of plastic in aqueous solutions demonstrated by CO2 evolution and quantification. *International Journal of Molecular Sciences*, 21(4), 1176. Available from: https://doi.org/10.3390/ijms21041176

Rummel, C.D., Lechtenfeld, O.J., Kallies, R., Benke, A., Herzsprung, P., Rynek, R. et al. (2021) Conditioning film and early biofilm succession on plastic surfaces. *Environmental Science & Technology*, 55(16), 11006–11018. Available from: https://doi.org/10.1021/acs.est.0c07875

Sauer, K., Stoodley, P., Goeres, D.M., Hall-Stoodley, L., Burmølle, M., Stewart, P.S. et al. (2022) The biofilm life cycle–expanding the conceptual model of biofilm formation. *Nature Reviews. Microbiology*, 20(10), 608–620. Available from: https://doi.org/10.1038/s41579-022-00767-0

Schefer, R.B., Armanious, A. & Mitrano, D.M. (2023) Eco-Corona formation on plastics: adsorption of dissolved organic matter to pristine and photochemically weathered polymer surfaces. *Environmental Science & Technology*, 57(39), 14707–14716. Available from: https://doi.org/10.1021/acs.est.3c04180

Schlundt, C., Mark Welch, J.L., Knochel, A.M., Zettler, E.R. & Amaral-Zettler, L.A. (2020) Spatial structure in the "Plastisphere": molecular resources for imaging microscopic communities on plastic marine debris. *Molecular Ecology Resources*, 20(3), 620–634. Available from: https://doi.org/10.1111/1755-0998.13119

Silva, L., Calleja, M.L., Huete-Stauffer, T.M., Ivetic, S., Ansari, M.I., Viegas, M., & Morán, X.A.G. (2019) Low abundances but high growth rates of coastal heterotrophic bacteria in the red sea, *Frontiers in Microbiology*, 9. Available from: https://www.frontiersin.org/articles/10.3389/fmicb.2018.03244 [Accessed 29th December 2023].

Sprouffske, K. (2020) Growthcurver package. https://cran.r-project.org/web/packages/growthcurver/vignettes/Growthcurver-vignette.html Accessed 31st January 2024.

Sprouffske, K. & Wagner, A. (2016) Growthcurver: an R package for obtaining interpretable metrics from microbial growth curves. *BMC Bioinformatics*, 17(1), 172. Available from: https://doi.org/10.1186/s12859-016-1016-7

Stamatakis, A. (2014) RAxML version 8: a tool for phylogenetic analysis and post-analysis of large phylogenies. *Bioinformatics*, 30(9), 1312–1313. Available from: https://doi.org/10.1093/bioinformatics/btu033

Stanier, R.Y., Palleroni, N.J. & Doudoroff, M. (1966) The aerobic pseudomonads: a taxonomic study. *Journal of General Microbiology*, 43(2), 159–271. Available from: https://doi.org/10.1099/00221287-43-2-159

Sudhakar, M., Priyadarshini, C., Doble, M., Sriyutha Murthy, P. & Venkatesan, R. (2007) Marine bacteria mediated degradation of nylon 66 and 6. *International Biodeterioration & Biodegradation*, 60(3), 144–151. Available from: https://doi.org/10.1016/j.ibiod.2007.02.002

Sun, Y., Wu, M., Zang, J., du, L., Huang, M., Chen, C. et al. (2023) Plastisphere microbiome: methodology, diversity, and functionality. *iMeta*, 2(2), e101. Available from: https://doi.org/10.1002/imt2.101

Taxonomy ID 236097. (n.d.) *(taxonomy_id:236097)peroxidase in UniProtKB search (15) | UniProt*. https://www.uniprot.org/uniprotkb?query=%28taxonomy_id%3A236097%29peroxidase Accessed 5th January 2024.

Tetu, S.G., Sarker, I., Schrameyer, V., Pickford, R., Elbourne, L.D.H., Moore, L.R. et al. (2019) Plastic leachates impair growth and oxygen production in *Prochlorococcus*, the ocean's most abundant photosynthetic bacteria. *Communications Biology*, 2(1), 1–9. Available from: https://doi.org/10.1038/s42003-019-0410-x

Tiso, T., Winter, B., Wei, R., Hee, J., de Witt, J., Wierckx, N. et al. (2022) The metabolic potential of plastics as biotechnological carbon sources – review and targets for the future. *Metabolic Engineering*, 71, 77–98. Available from: https://doi.org/10.1016/j.ymben.2021.12.006

Tiwari, N., Santhiya, D. & Sharma, J.G. (2022) Biodegradation of micro sized nylon 6, 6 using *Brevibacillus brevis* a soil isolate for cleaner ecosystem. *Journal of Cleaner Production*, 378, 134457. Available from: https://doi.org/10.1016/j.jclepro.2022.134457

Tiwari, N., Santhiya, D. & Sharma, J.G. (2024) Significance of landfill microbial communities in biodegradation of polyethylene and nylon 6,6 microplastics. *Journal of Hazardous Materials*, 462, 132786. Available from: https://doi.org/10.1016/j.jhazmat.2023.132786

Tokiwa, Y., Calabia, B.P., Ugwu, C.U. & Aiba, S. (2009) Biodegradability of plastics. *International Journal of Molecular Sciences*, 10(9), 3722–3742. Available from: https://doi.org/10.3390/ijms10093722

Wallbank, J.A. et al. (2022) Into the Plastisphere, where only the generalists thrive: early insights in Plastisphere microbial community succession. *Frontiers in Marine Science*, 9. Available from: https://doi.org/10.3389/fmars.2022.841142 Accessed 20th December 2023.

Wang, S., Lydon, K.A., White, E.M., Grubbs, J.B., III, Lipp, E.K., Locklin, J. et al. (2018) Biodegradation of poly(3-hydroxybutyrate-co-3-hydroxyhexanoate) plastic under anaerobic sludge and aerobic seawater conditions: gas evolution and microbial diversity. *Environmental Science & Technology*, 52(10), 5700–5709. Available from: https://doi.org/10.1021/acs.est.7b06688

Wik, T. (2003) Trickling filters and biofilm reactor modelling. *Reviews in Environmental Science and Biotechnology*, 2(2), pp. 193–212. Available from: https://doi.org/10.1023/B:RESB.0000040470.48460.bb

Wright, R.J., Bosch, R., Langille, M.G.I., Gibson, M.I. & Christie-Oleza, J.A. (2021) A multi-OMIC characterisation of biodegradation and microbial community succession within the PET plastisphere. *Microbiome*, 9(1), 141. Available from: https://doi.org/10.1186/s40168-021-01054-5

Wright, R.J., Langille, M.G.I. & Walker, T.R. (2021) Food or just a free ride? A meta-analysis reveals the global diversity of the Plastisphere. *The ISME Journal*, 15(3), 789–806. Available from: https://doi.org/10.1038/s41396-020-00814-9

Yakimov, M.M., Bargiela, R. & Golyshin, P.N. (2022) Calm and frenzy: marine obligate hydrocarbonoclastic bacteria sustain

ocean wellness. *Current Opinion in Biotechnology*, 73, 337–345. Available from: https://doi.org/10.1016/j.copbio.2021.09.015

Yoon, S.-H., Ha, S.M., Kwon, S., Lim, J., Kim, Y., Seo, H. et al. (2017) Introducing EzBioCloud: a taxonomically united database of 16S rRNA gene sequences and whole-genome assemblies. *International Journal of Systematic and Evolutionary Microbiology*, 67(5), 1613–1617. Available from: https://doi.org/10.1099/ijsem.0.001755

Zadjelovic, V., Erni-Cassola, G., Obrador-Viel, T., Lester, D., Eley, Y., Gibson, M.I. et al. (2022) A mechanistic understanding of polyethylene biodegradation by the marine bacterium *Alcanivorax*. *Journal of Hazardous Materials*, 436, 129278. Available from: https://doi.org/10.1016/j.jhazmat.2022.129278

Zettler, E.R., Mincer, T.J. & Amaral-Zettler, L.A. (2013) Life in the "Plastisphere": microbial communities on plastic marine debris. *Environmental Science & Technology*, 47(13), 7137–7146. Available from: https://doi.org/10.1021/es401288x

Zhang, Y., Cao, Y., Chen, B., Dong, G., Zhao, Y. & Zhang, B. (2024) Marine biodegradation of plastic films by *Alcanivorax* under various ambient temperatures: bacterial enrichment, morphology alteration, and release of degradation products. *Science of the Total Environment*, 917, 170527. Available from: https://doi.org/10.1016/j.scitotenv.2024.170527

How to cite this article: Mattelin, V., Rombouts, A., Van Landuyt, J., Scoma, A. & Boon, N. (2024) Specialization of *Alcanivorax* species in colonizing diverse plastics. *Environmental Microbiology*, 26(10), e16698. Available from: https://doi.org/10.1111/1462-2920.16698

APPENDIX: METHODS FOR PLASTIC-ENRICHED MICROBIAL COMMUNITIES A

To enrich microorganisms with the capability to degrade plastics, the indigenous microbiome of the North Sea was incubated with plastics as the sole carbon source. Seawater was collected at the coast in Ostend, Belgium (51°10′31.1″ N; 3°14′00.6″ E) on the 22nd of January 2020. The seawater was incubated with 1 g/L of plastic (PHBH, PA 6/69 and B4PF01) and every 4 weeks, 10% of the microbial community was transferred to a new flask containing 22.5 mL of either mineral salts medium or 10× diluted ONR7a medium and 1 g/L plastic. The flasks were incubated at 20°C. DNA samples from both the plastisphere bacteria and the planktonic cells were taken after 7 transfers (31 weeks).

To promote biofilm growth, trickling filter bioreactor systems were used. Trickling filters are very commonly used bioreactor systems that allow dense biofilm growth due to the great void space, high porosity (thus aeration) and higher hydraulic loading (Parker et al., 1997; Wik, 2003; Buchanan, 2014). The trickling filter was designed with in-house made, small, PVC cylindrical reactors (diameter 5 cm and height 8 cm). The reactors were filled for 80% with plastic granules (two replicates with B4PF01 polymer, referred to as F1 and F2 reactors), with the remaining volume left open for air

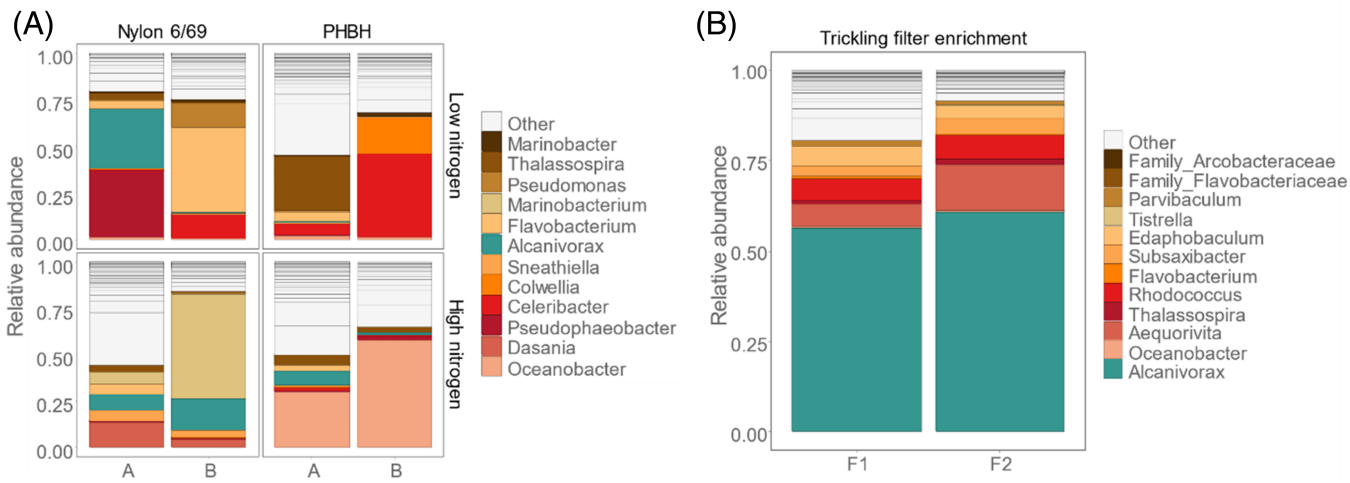

FIGURE A1 16S rRNA gene amplicon sequencing. The relative abundance of the top 12 genera, based on ASVs of the nylon 6/69, PHBH and B4PF01 incubations of the plastic-enriched communities (A) flask enrichment and (B) trickling filter enrichment, used as inoculum in this follow-up experiment. More information on experimental procedures of enrichment is in Appendix A.

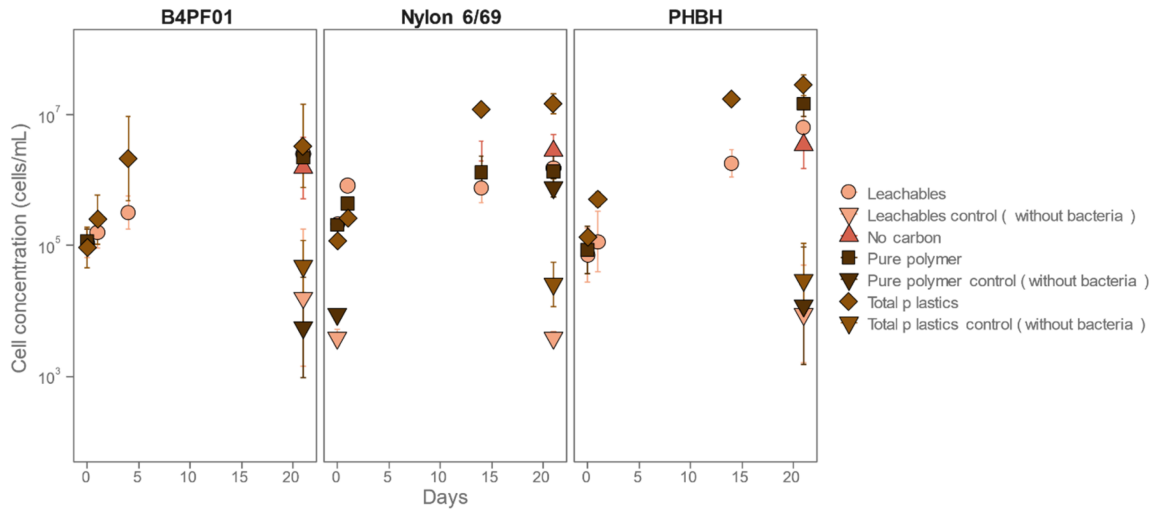

FIGURE A2 Cell growth of plastic-enriched communities on different types (B4PF01, nylon 6/69 and PHBH) and material fractions (leachables, pure polymer and plastic (i.e., leachables + polymer)) of plastics during 21 days ($n = 3$, three technical replicates per biological triplicate as mean value, including standard deviation). Leachables/polymer/plastic control indicates the incubation without microorganisms, and 'no carbon' indicates the incubation of the microbial community without an added (plastic) carbon source.

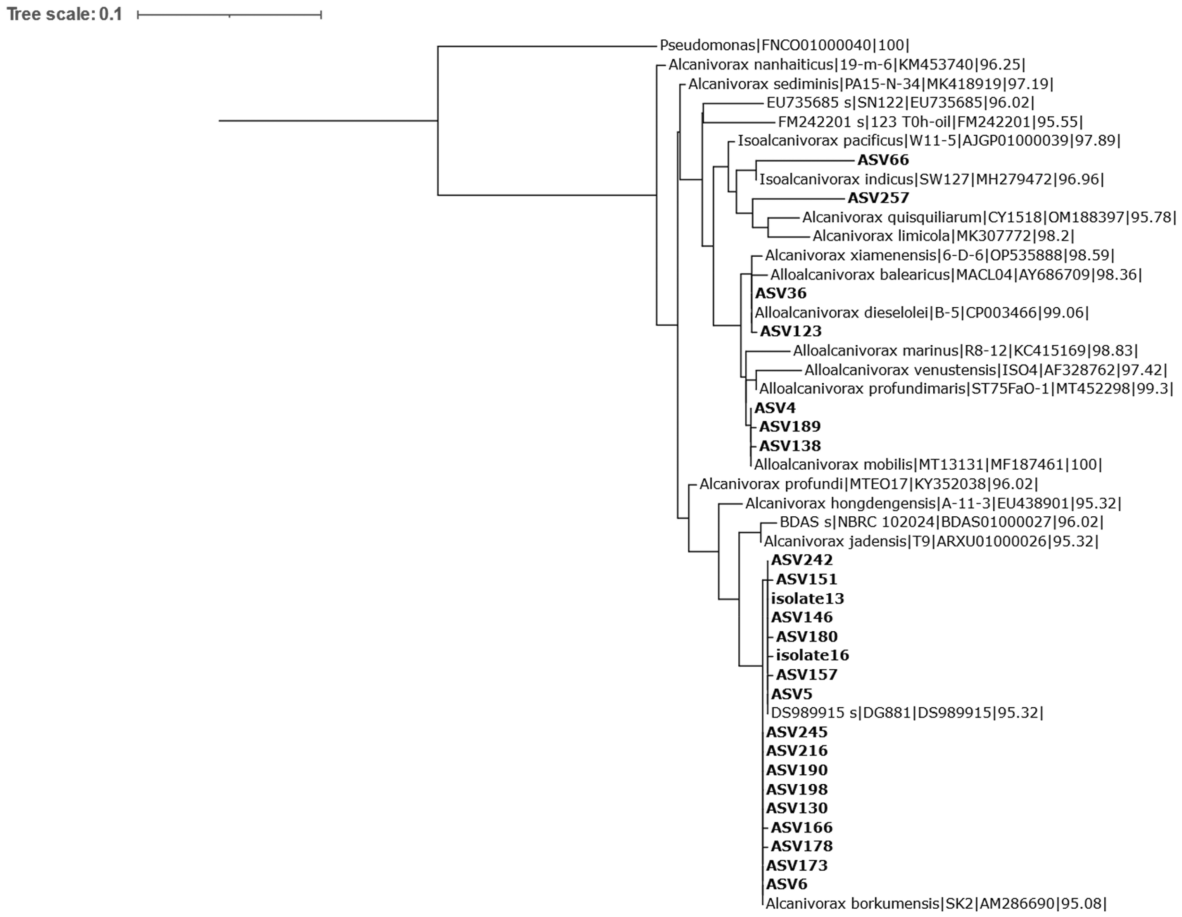

FIGURE A3 Phylogenetic tree placing the short 16S rRNA gene amplicon sequencing reads in a reference tree, consisting of long 16S type strain sequences.

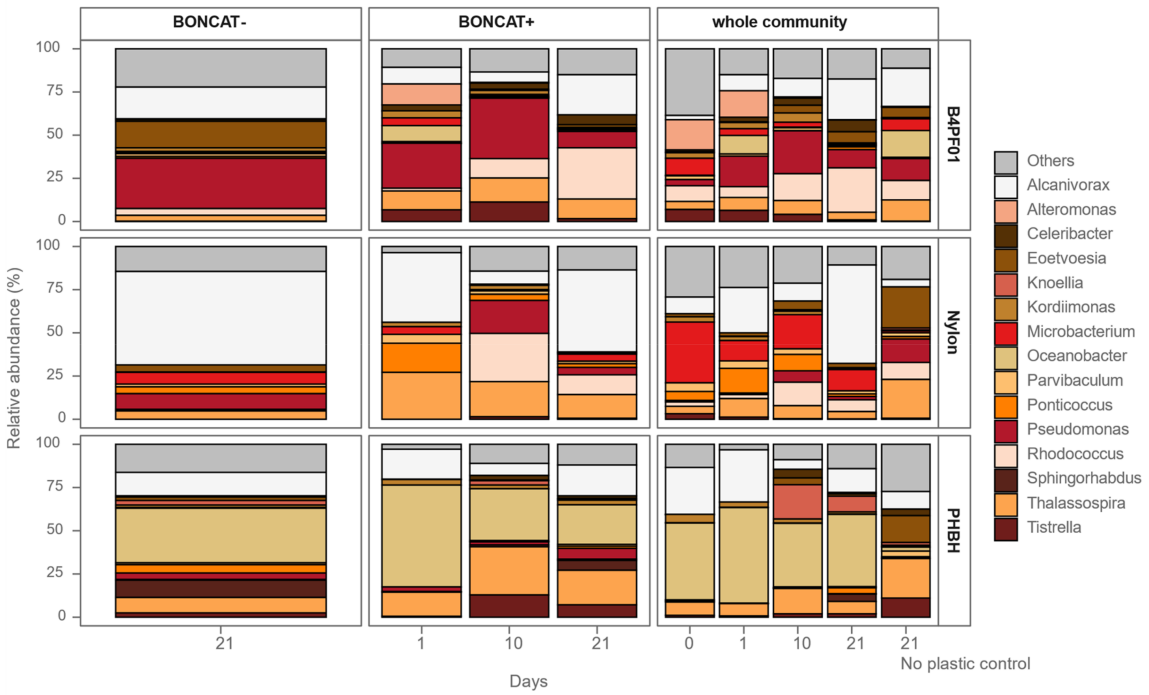

FIGURE A4 16S rRNA gene amplicon sequencing. Relative abundance of the top 15 genera based on ASVs. Samples include the whole community, the BONCAT+ and BONCAT− FACS-sorted populations.

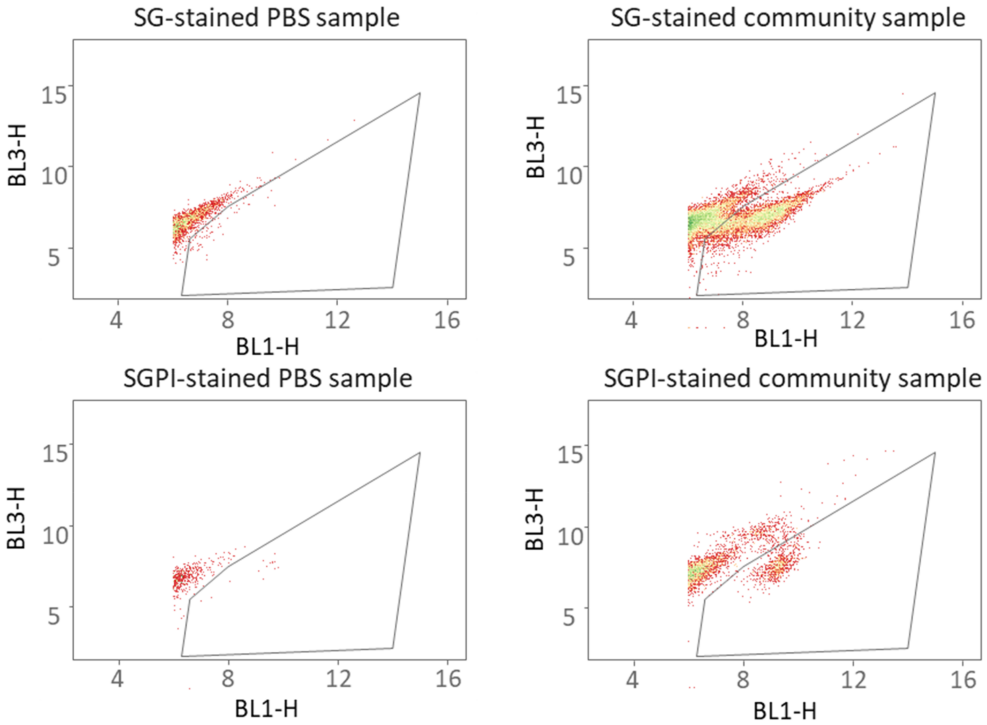

FIGURE A5 Gating strategy of flow cytometry data stained by either Sybr Green I (distinguishes cells from background) or Sybr Green I + propidium iodide (distinguished damaged cells and background from intact cells). BL1-H indicates the blue laser (488 nm) and first detector (530/30 nm) (height value) and measures green fluorescence. BL3-H indicates the blue laser (488 nm) and the third detector (695/40) (height value) and measures red fluorescence.

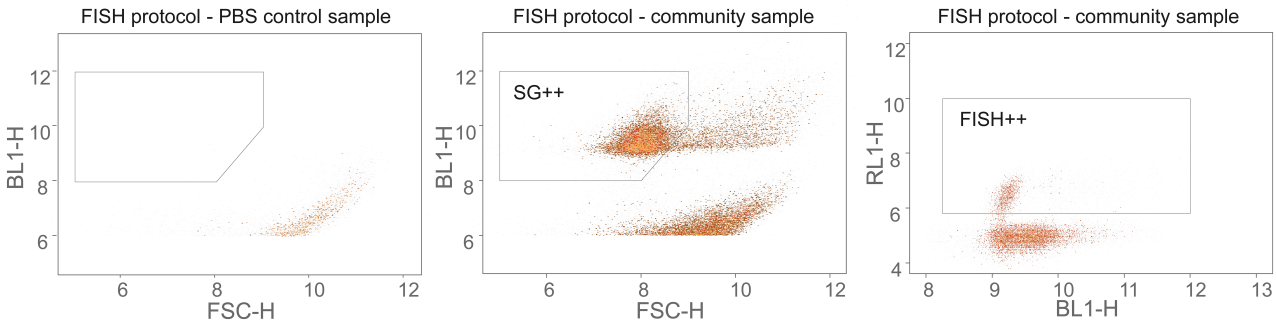

FIGURE A6 Gating strategy for FISH stained cells. Left: PBS control sample included in the full protocol; middle: discrimination between SG stained cells (all cells) and the background; right: discrimination between the FISH stained (filtered) cells and the non-FISH labelled. FSC-H indicates the forward scatter (height value). BL1-H indicates the blue laser (488 nm) and first detector (530/30 nm) (height value) and measures green fluorescence. RL1-H indicates the red laser (647 nm) and the first detector (670/14 nm) (height) and measures red fluorescence.

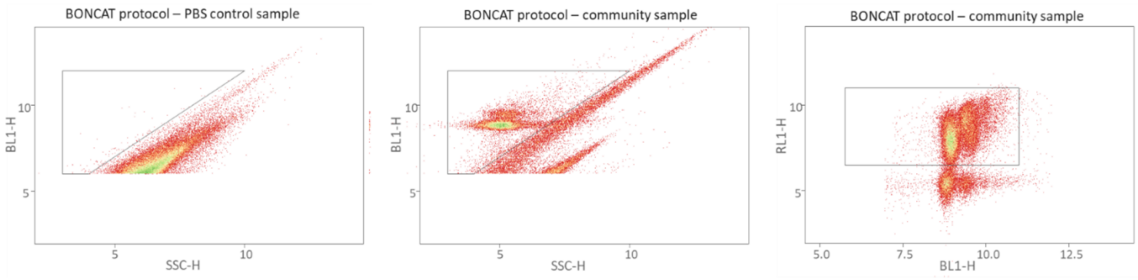

FIGURE A7 Gating strategy for BONCAT stained cells. Left: PBS control sample included in the full protocol; middle: discrimination between SG stained cells (all cells) and the background; right: discrimination between the BONCAT stained (filtered) cells and the non-BONCAT labelled. SSC-H indicates the sideward scatter (height value). BL1-H indicates the blue laser (488 nm) and first detector (530/30 nm) (height value) and measures green fluorescence. RL1-H indicates the red laser (647 nm) and the first detector (670/14 nm) (height) and measures red fluorescence.

supply. A schematic overview is shown below. Mineral salt medium was trickled over the plastics at a rate of 6 mL/min which resembled a dripping speed. The trickling filter system was set up in a controlled temperature room at 15°C. The media was initially inoculated with a mixed culture obtained in previous enrichments, in an amount of 10^6 cells/mL. The reactors were run in batch mode, and every 2 or 1 week(s), fresh mineral salt media was supplied and inoculated with 10% of the previous batch. Plastisphere and effluent samples for amplicon sequencing were taken at the end of each batch. The reactors were run for 5 batches, with corresponding sampling points at 0, 14, 28, 35, 42 and 56 days for DNA sequencing.

in drinking water, only a small fraction (0.1%–9%) of the total organic carbon (TOC) is assimilable organic carbon, although still a very important factor governing heterotrophic growth (Hammes & Egli, 2005). The medium used in this study had a measured 403 μg/L DOC. Assuming the carbon requirement for microbial growth can be estimated as 1 ppm DOC per 10^6 cells/mL, it could be estimated that this would result in microbial growth of 1.8×10^3 to 1.6×10^5 cells from the medium alone in this study. This is supported by the decrease in DOC for the pure polymer incubations of B4PF01 and nylon 6/69 (Figure 9). Our results furthermore confirm heterotrophic growth in the pure medium when no carbon source was added for both

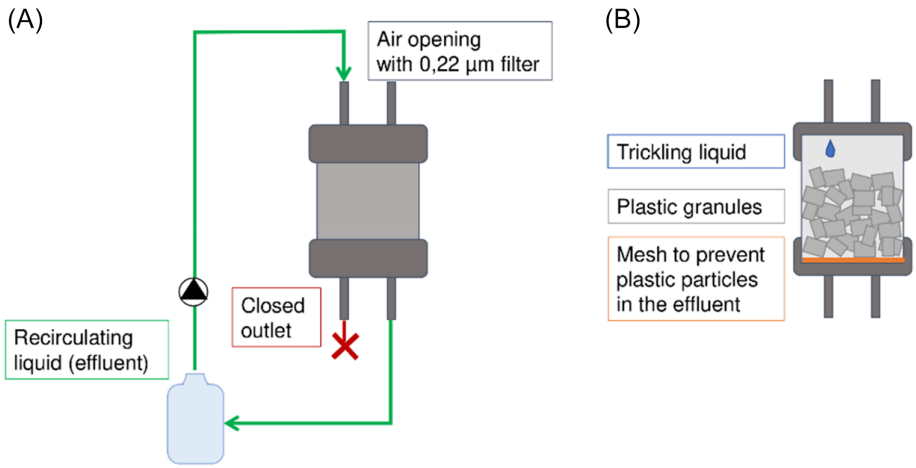

APPENDIX: MICROBIAL GROWTH IN VERY LOW CARBON CONCENTRATIONS B

Marine microorganisms are used to oligotrophic conditions and are described to grow on limited carbon supply at high growth rates (Silva et al., 2019). In addition, copiotroph bacteria are present, that can thrive at high carbon concentrations (Lauro et al., 2009). When working with recalcitrant carbon sources such as plastic, unwanted carbon contamination can influence (selective) microbial growth and give misleading results. Practically, working completely carbon-free is very difficult, as many manipulations, such as autoclaving, generally add unwanted low concentrations of carbon to the medium (Andersson et al., 2018). It is reported that, the microbial communities and the isolates (Figures 2 and 8). The carrying capacity for the *A. borkumensis*-like isolate was calculated to be lower for B4PF01 and nylon 6/69 compared to the control (Table 3). Although the fluorescence indicates that PHBH is biodegraded, with the highest degradation by the community, followed by *A*. DG881-like isolate and *A. borkumensis*-like isolate, at the end of the PHBH plastic incubation, the growth parameters are similar for the plastic and control, confirming very low rates of plastic biodegradation by the isolates. For the microbial communities, the carrying capacity is higher compared to the control without carbon (Table 1). The lower carrying capacity for the isolates on nylon 6/69 and PHBH could confirm the complexity of plastic biodegradation.